Development and evaluation of a polyethylene knee insert with integrated wear sensors

N.M. Dinaux

TU Delft Delft University of Technology

TNO innovation for life

Development and evaluation of a polyethylene knee insert with integrated wear sensors

MSc Thesis

by

N.M. Dinaux

in partial fulfillment of the requirements for the degree of

Master of Science
Biomedical Engineering, biomaterials and tissue biomechanics track

at the Delft University of Technology,
to be defended publicy on Thursday September 27, 2018 at 01:30 PM.

Supervisors:	Dr. J. Zhou	
	Mr. R. Reese	
Thesis committee:	Dr. J. Zhou,	TU Delft
	Dr. ir. M. Hermans	TU Delft
	Dr. ir. T. Horeman	TU Delft
	Mr. F. Bruning, Msc	TNO

SUMMARY

Currently, measuring wear of the insert of knee implants can only be accurately done in vitro. There are yet no accurate in vivo techniques that can capture and deliver data in real time. Therefore, the main objective of the research reported in this thesis was to introduce and validate a polyethylene insert with integrated wear sensors into knee implants that could be used in vivo after total knee replacement surgery. The instrumented insert was expected to help physicians and patients to acquire accurate wear information about the knee implant for an objective outcome evaluation of the intervention and to help to prevent excessive implant deterioration over time.

A mechanical test setup with different parts of a knee implant was built. First, the positions where the highest forces would act on the implants, were determined by integrating resistance sensors in the test setup. The results of this test were used to determine the positions of the wear sensors, since the tibiofemoral forces correlate with the amount of the wear of the insert. Then, the insert with integrated wear sensors was produced by filling six cutouts in the insert with silver conductive paint and creating six tracks in three different layers. When the resistance of the track would be infinite, the track should be worn-out. This prototype was tested in the same test setup.

The resistance values of the conductive tracks were measured to range from 40.3 to 128.4 Ω. After 6732 and 9974 cycles, the highest track on the medial and lateral sides, respectively, became damaged by the moving femoral head. The resistance of the tracks rose immediately to be infinite. Measuring the wear track with a caliper gave a value of 0.65 mms, which was deeper than the pre-determined track depth. The following tracks gave similar results.

One of the limitations of the present study concerned the movement of the knee. Since the test setup was only made of a hinge, it could not be compared with a whole knee movement that also contains translation. Thereby was the prototype only suited for in vitro tests due to the materials choice and lack of a data transmitter. Since the prototype was made by hand, the layer thickness could not exceed the minimum of 0.6 mm and were the layers glued on each other. This made the wear measuring method not as accurate as wished. Nevertheless, the wear pattern corresponded well with the expected wear caused by the tibiofemoral forces.

All in all, the insert with integrated silver conductive tracks is a concept that can be translated into a good solution to measuring wear in vivo in the near future. For the further development of this concept, the insert should be printed completely on a 3D printer. Thereby, more research should be performed on materials that could be used as conductive tracks, the possibilities to integrate more wear sensors to measure wear more accurately and the transmission of signals.

LIST OF ABBREVIATIONS

Abbreviation	Composition
3D	3 dimensional
BW	Body weight
CMMs	Coordinate measuring machines
EMG	Electromyography
micro-CT	Micro computed tomography
OA	Osteoarthritis
PE	Polyethylene
PEN	Polyethylene naphthalate
TKR	Total knee replacement
UHMWPE	Ultra-high molecular weight polyethylene

CONTENTS

INTRODUCTION

Total knee replacement is a surgical procedure, in which parts of the knee joint are replaced with artificial parts. According to the Dutch Arthroplasty Register, the LROI, more than 24,000 total knee replacements are performed each year in the Netherlands [1]. In addition, about 3,000 knee revisions are performed each year [1]. In the USA the number of total knee replacements that is performed each year is more than 600,000 plus about 22,000 revisions [2]. Wear of the insert is an important factor for these revisions. Understanding the wear and its pattern will surely contribute to reducing the number of revision surgeries.

Knee joint

The knee is the most complex joint in the body. The knee is actually a hinge joint, which means that it can bend, straighten and twist. However, the knee is not just as simple as a hinge. The knee has six degrees of freedom: it can rotate on three different axes and it can translate in three directions, as illustrated in Figure 1.

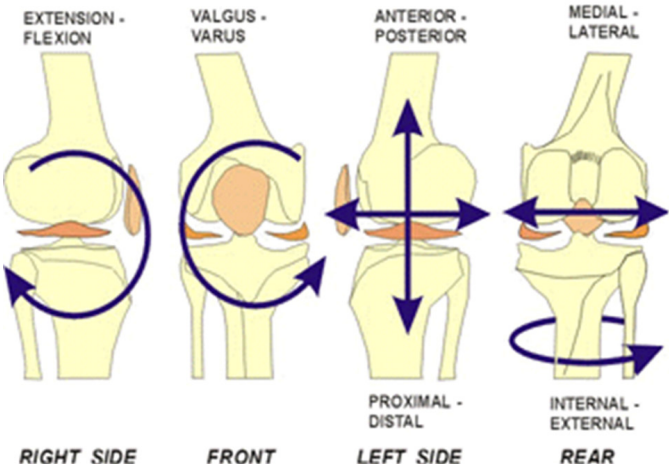

Figure 1 – The six degrees of freedom of the knee joint [76].

Osteoarthritis

Osteoarthritis (OA) is a condition, in which the natural cushioning between joints wears away. When this happens, the bones of the joints rub closely against one another with less of the shock-absorbing benefits of the cartilage. The rubbing results in pain, swelling, stiffness and decreased ability to move.

OA is the most common type of arthritis. One of the major risk factors for knee OA is age; the chance of developing OA rises after age 45 [3]. However, young people can suffer from it as well. For some, it can be hereditary, but others have OA resulting from an injury, infection or being overweight. Almost everyone will eventually develop some degree of OA due to ageing. However, several factors increase the risk of developing significant OA at an earlier age, such as heavy weight, heredity, repetitive stress injuries, such as kneeling, high intensity athletics or other illnesses, such as rheumatoid arthritis [4].

Women are more likely to have OA than men. The exact causes for this are still unknown, however a few studies have shown that the anatomy and hormones have effects on the development of OA. Women's broader hips may put more long-term stress on their knees. It is generally believed that estrogen protects cartilage from inflammation. When the estrogen levels go down after the menopause, women are more prone to develop OA [4].

Malalignment of the lower extremity, which overloads one compartment at the expense of another is also associated with progression of OA. Motion analysis studies, which calculate the external moments of the knee, have correlated an increased peak adduction moment

at the knee with pain, radiographic progression and biomarkers of disease severity. While these changes in adduction moment are subtle, as little as 3° to 5° of increased tibial varus alignment (as shown in Figure 2) can induce a 50% increase in the force transmitted across the medial tibiofemoral compartment [5].

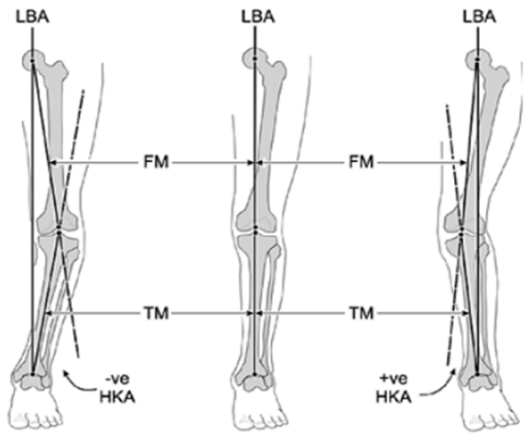

Figure 2 – Knee position. Left: varus. Middle: neutral. Right: valgus [81].

Total knee replacement

The only effective treatment for end-stage OA is knee arthroplasty, also known as total knee replacement (TKR). OA is the main reason why TKRs are performed (Figure 3). Knee replacement surgery was, for the first time, performed in 1968. Since then, improvements in surgical materials and techniques have greatly increased its effectiveness.

Indications for surgery	Percentage
Osteoarthritis	98%
Avascular necrosis	<1%
Inflammatory arthropathy	<1%
Previous infection	<1%
Rheumatoid arthritis	1%
Previous trauma	<1%
Other	<1%

Figure 3 – Reasons for TKR [3].

Knee implant

Generally, the knee implant is composed of three parts: the tibial component, the insert (or spacer) and the femoral component, as can be seen in Figure 4. The tibial and femoral components are respectively attached to the tibia and femur. The shape of these components can differ per implant manufacturer. There are different types of fixation used to attach the implant to the bones, such as cemented and cementless fixation. Which implant a patient will get, depends on several factors, such as the progression of OA, the health of the ligaments and the preference of the surgeon. In addition, there are different implant designs that retain different ligaments. The choice differs again per patient and per surgeon.

Thereby can the materials of the implants vary as well. The metal parts of the implants are mostly made of titanium or cobalt-chromium-based alloys. The insert is practically always made of a thermoplastic polyethylene (PE): ultra-high molecular weight polyethylene (UHMWPE). Some implants are made of ceramics or ceramic with metal mixtures (composites). The choice of the material is dependent of the manufacturer.

Since 1994, the trend has changed and the mean age for the primary TKR has decreased. In 2012, it was around 68 [6]. This change in the trend seems to be strange, but it is justified, considering the fact that obesity, one of the biggest causes for knee OA, has increased in the new generations in the developed countries. Moreover, the increasing number of people practicing sport at a high level has also increased the injury rate and the necessity for a knee prosthesis at a young age.

How long a knee replacement lasts in a patient depends on several factors, including activity level, body weight (BW) and general health. Just like wear in the natural joint that leads to the need for a replacement, wear in the implant may eventually require a second surgery, which is called joint revision. The life expectancy of a knee prosthesis inside the human body is around 15-20 years. A recent study conducted by Bae at al. on 224 patients who needed

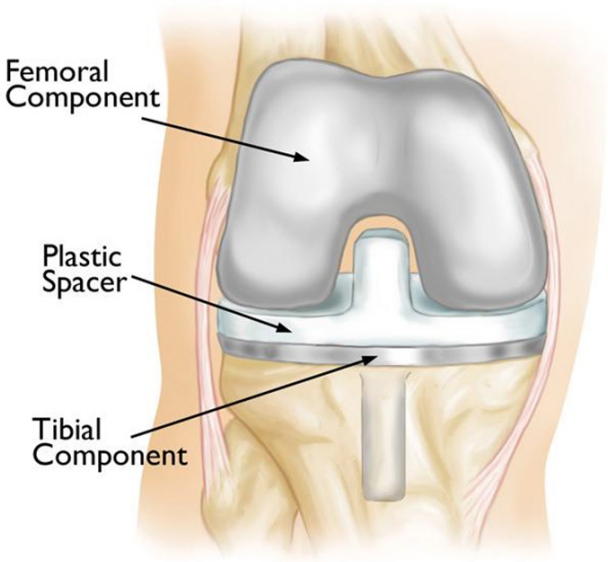

Figure 4 – Components of a knee implant [77].

revision surgeries from 1999 to 2009 showed that the survival rates prior to any revisions being necessary were 97% after 5 years, 92% after 8 years, and 86% after 10 years [7].

In a revision procedure, some or all of the parts of the original implants are removed and replaced with new components. Typically, revision components have longer stems which fit into the femur and tibia. They may also have attached metal pieces, called augments, which substitute for missing bone. Most of the time, the revision surgery is more thorough than the first total knee replacement. There are different reasons why a revision should be performed. These can be found in Figure 5.

In fact, a revision is more complex for the surgeon, the rehabilitation is longer for the patient and the whole treatment is more expensive for the national health service or insurance company. Considering the mean age of the first implant 68, the average life expectancy of the prosthesis 15 years and the life expectancy which is now around 80 years in the developed countries, the probability of a second revision surgery for the patient with a prosthesis implanted at a young age is not negligible.

Wear of the knee insert

As can be seen in Figure 5, wear is not the most important direct factor for a revision surgery. However, wear debris generated from bearing materials could cause aseptic loosening, osteolysis and at the end implant loosening and therefore is indirectly responsible for more revision surgeries [8], [9].

Many factors influence the amount of wear that occurs in the knee implant: patient-related, implant and surgical factors. Patient-related factors, such as BW and activity level, determine the amount and types of load experienced by the implant [10], [11]. Age can have an influence on the activity level of the patient. Activity level is likely the most important patient factor affecting the loads placed on the knee implant over time [12]. Implant factors are the material properties, such as the molecular weight, the area and roughness of the articular surface, and the thickness of the insert. The FDA (U.S. Food and Drug Administration) requires now that the insert has a thickness of more than 6 mm, since a thinner insert will exponentially increase contact stresses [13]. In practice, a minimum insert thickness of 8 mm and a maximum insert thickness of 16 mm are recommended [14]. Good surgical technique is also required to minimize PE wear in the knee implants. Poor alignment of knee components may occur at the time of surgery in the coronal, sagittal or rotational planes. Failure to restore the mechanical axis

Indications for surgery	Percentage
Aseptic loosening	32%
Pain	15%
Lysis	8%
Wear of polyethylene component	10%
Instability	14%
Infection	22%
Malalignment	6%
Stiffness	5%
Progressive arthritis remaining	9%
Dislocation/subluxation	3%
Periprosthetic fracture	3%
Component dissociation	2%
Implant fracture	<1%
Other	10%

Figure 5 – Reasons for knee implant revisions [3].

of the limb at the time of surgery may result in increased loading forces across the bearing surface, leading to early degradation of PE. Minor deviations from a neutral mechanical axis may contribute to accelerated wear, which is not evident until the implant has been functioning for many years.

It is still unknown how to design wear-resistant artificial joint parts and select ideal material pairs for TKR. Therefore, examining the wear characteristics of the prosthesis materials is still an interesting research area in in vitro laboratory simulations and for in vivo clinical applications.

Relation between tibiofemoral force and wear

Since body weight, activity level and certain knee movements contribute to the wear of the meniscus and the insert, it seems correct that contact stress and wear have a relationship with each other. D'Lima confirms that contact stresses are correlated with the magnitude and distribution of wear [15]. He states that tibial forces are related directly to the transmission of stresses in the implant, which include the contact stresses generated at the bearing surface. The stresses at the bearing surface are a major factor in generating wear and fatigue [16].

Knee forces are even more important after TKR surgery because unlike biological tissues, the materials used in the knee implant do not regenerate or remodel. Knee forces are therefore directly implicated in articular wear and damage, especially to the PE insert that fulfills the function of the meniscus in the knee implant.

Previous work

Many studies have been carried out to determine the tibiofemoral force: the compressive force that is a result of the ground reaction force plus antagonist muscle forces on the knee. This force is expressed in relation to bodyweight (x BW), since it is highly dependent on the weight of a person. Four methods have been used to determine this force: computational models, test setups, cadaver tests and in vivo tests.

Computational methods can be separated into three categories: optimization method, electromyography- (EMG-) driven method, and reduction method [17]. Each of them uses rigid multibody dynamics to model how movements are generated by the muscle forces.

In the test setups, different knee joint demonstrators have been developed for different studies [18]–[20]. These tests setups contain quite complex simulators, since most of the time all three rotational movements of the knee are integrated into such demonstrators. In these studies, force sensor films are glued on [18], [19] or integrated into the insert [20] to measure the tibiofemoral force.

Most recent cadaver studies use nested cylinders supporting the tibial plateau to measure multiaxial forces and moments in cadavers. The force sensors in these studies are also glued on [21], [22] or integrated into the insert [23].

The in vivo studies use a so-called "instrumented implant", into which several sensors are integrated. Forces can be measured in vivo. All the studies that have been conducted with an instrumented implant in vivo, use an instrumented tibial tray. Clear reasons for this are not given, but probable reasons are that there is more space in the tibial tray and the insert is more prone to wear, and as a result the sensors can be affected.

The studies that determine the tibiofemoral force are performed because it can tell something about the wear rate of the meniscus or the insert [15], [16], [24]–[45]. However, none of these studies report the wear of the polyethylene insert. A number of studies specifically on the linear wear rate of an insert have been carried out [46]–[59]. Although several reliable methods for measuring PE wear in total hip replacements (THR) exist, the methods for accurate measurement of PE wear after TKR have only recently been developed. The methods and the relevant studies are described below.

The gravimetric method is the

Figure 6 – Gravimetric machine [78].

Figure 7 – Coordinate measuring machine [79].

standardized method for quantifying wear volumes of total joint prosthesis (Figure 6). In this method, specimen weight is measured before and after wear test and the difference of the two measurement values are calculated. However accurate results it gives, this method can only be applied during in vitro testing of new prostheses. It does not give any information about the worn surfaces and plastic deformation of the implant material. If there is a lack of initial weight measurement values, it is not possible to define the wear of retrieved implants. This method was used in a recent in vitro study performed by Srivastava et al [51] to determine the alignment of the implant and its relationship with increased wear.

Coordinate measuring machines (CMMs) can measure the dimensions with tactile probe or scanning probe (Figure 7). This is one of the geometry-based methods that can be used for evaluating both wear volume and wear distribution over the worn surface. For defining the quantity of the wear, it requires unworn reference geometry of the prosthesis for comparing it with worn geometry. In wear simulator studies, the geometry of the specimen is defined before and after the wear test and then the results are compared for evaluating the wear. In the studies of Harman (2009) and Kop (2007) inserts retrieved from patient were used [49], [50]. The measured wear rates in these studies were 0.29 mm/year [50] and 0.053 mm/year [49], respectively. Generally, it is quite hard to execute this method on retrieved inserts, since the exact measurements of the pre-worn implant should be available. Besides wear measurements, the CMM method provides volumetric and linear creep measurements.

A simplification of the CMMs is a dial gauge. This measuring device is most of the time operated by hand and gives less extensive data than CMMs. Since the dial gauge is an easy accessible tool, a lot of studies have been carried out with this method [46], [47], [53]–[55], [60]. Every study showed the linear wear rate that differed from 0.025 mm/year [47] to 0.127 mm/year [55]. And others also determined the volumetric wear rate [53], [55].

The micro computed tomography (micro-CT) technique uses X-rays to generate three-dimensional (3D) geometries of the implants (Figure 8). By using a calibrated X-ray detector, the implants are scanned with the patient standing, and the data are processed by computer to measure the distance between the femoral head and the tibial baseplate. Currently, this is the only method to measure wear in vivo. Several studies have been carried out to measure the wear rate in vivo with micro-CT [48], [56], [57], [59]. The minimum linear wear rate measured by Price (2005) was 0.021 mm/year [59]. The maximum linear wear rate measured in the study of Hoshino was 0.23 mm/year [56]. This method provides reliable and accurate measurement of the wear of PE, but it is a very expensive method and has some difficulties to distinguish actual wear amount from creep. Moreover, simple asymmetry of the joint space on

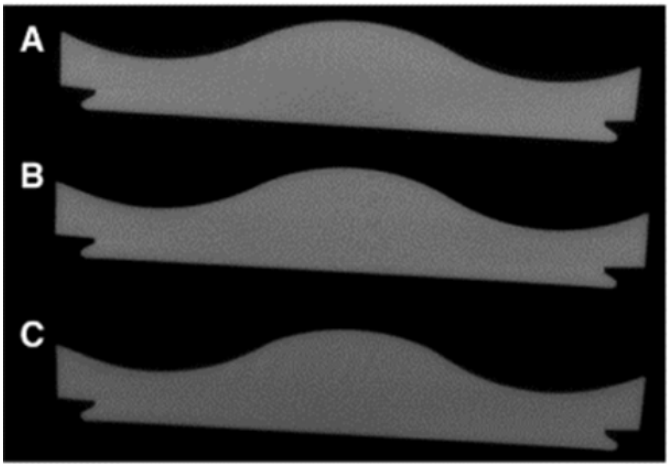

Figure 8 – Example of an insert visualized by micro-CT [80]

TKR radiographs does not necessarily prove that PE wear is present, because ligamentous laxity on one side of the knee may appear as joint-space narrowing in the opposite compartment [61].

The average linear wear rate of all the studies mentioned above was 0.12 mm/year. Some researchers also measured the wear rate difference between the medial and lateral side of the insert [47], [51], [52], [57], [58], [62]. In these studies, differences between the wear of the medial side and wear of the lateral side were found, but none of them was significant. Plante-Bordeneuve showed in his study that the difference in the wear of the medial and lateral compartments was linearly related to the alignment of the knee, with greater medial wear in varus knees and vice versa [47].

Societal relevance and motivation

The purposes of TKR are primarily to relieve pain and recover the mobility of the patient. Even though over 1 million knee joints are implanted each year in the EU and US, almost none provide feedback to allow early diagnosis of any fault with the implant [63]. Using such feedback, the physicians will have a set of quantitative measurements that will help in the identification of the defects. Consequently, they will be able to improve rehabilitation and modify treatments. Such feedback can also provide knowledge about the biomechanics of joints and the basis for possible modifications for future prostheses. Therefore, the feedback information is of great significance, especially if this can be collected in normal daily conditions.

Since a revision surgery is complex and highly invasive, it is desirable if such a surgery can be avoided. An instrumented insert with wear sensors will help the physicians and patients to have accurate information about the wear of the implant for an objective outcome evaluation of the intervention and to prevent excessive implant deterioration. The possibilities to measure wear in vivo are currently very limited and there is room for improvement. In the research reported in this thesis, a new concept of linear wear measurement that could possibly be used in vivo, was developed and tested.

Research question and objectives

The main objective of this research was to introduce a PE insert with integrated wear sensors that could eventually be used in vivo.

This objective resulted in the following research question: are instrumented inserts with integrated linear wear sensors an effective solution to measuring implant deterioration in vivo?

To answer this research question, the following three sub-objectives were defined:

- Determine the ideal position for wear sensors
- Develop a prototype with integrated wear sensors
- Validate the functionality of the prototype

Thesis structure

This thesis describes the development and evaluation of an additively manufactured knee insert which can measure linear penetration wear. In the first part of the Materials and Methods section the design criteria and the design of the insert with integrated wear sensors is detailed. The second part describes the tests which were carried out to validate the performance of the insert.

In Results, the outcomes of the position determination are shown and then the validation of the insert is elaborated.

In Discussion, the results of each test are reflected upon and consideration is given to how these outcomes will affect the insert. Furthermore, the possibilities are explored for the prototype to better meet the requirements and

wishes that are defined earlier in the process.

The overall successfulness of the designed insert is evaluated in Conclusion. Afterwards, recommendations for future research are given.

MATERIALS AND METHODS

Wear measuring technique

3D printing is a manufacturing technique where the product is built layer by layer. It opens up the possibilities to integrate wear sensors in the insert. In the 3D printing process, different layers of the insert contain a track of a conductive material. If a resistance value through the wire can be measured, the track is intact. However, when the resistance is infinite, the track is broken. Since the tracks are covered by a stiff layer of PE, it is only possible that the tracks break when the material has worn down. Since the tracks are positioned at different pre-determined heights inside the insert, it is possible to determine the exact amount of the linear penetration wear of the insert.

Design process

To create a suitable prototype, several steps were taken. First the design criteria were defined. These design criteria were critical for the further design of the insert. To meet the first research sub-objective, i.e., determining the optimal position of wear sensors, first a "bare" insert was created. With this insert, different forces acting on the surface of the insert were measured during the knee movement. Based on this data, the positions of the wear sensors were determined. Then, the prototype with integrated wear sensors was created and tested with the same knee movement test setup.

Design criteria

Before designing the insert, the requirements and wishes were listed. The requirements were actually the criteria that would have to be met in order to reach an acceptable solution.
Wishes were the criteria that would not necessarily have to be met but could be used later on for elaborating the concept. Setting up the program of requirements and wishes was a continuous and iterative process, as during the project the criteria became more numerous and more specific.

Before this list was made, several assumptions were made. This was because this prototype design would fulfill the function of an in vitro testing prototype but not be used for in vivo tests as yet. This means that some simplifications could be made, and the approval for testing in a laboratory setting would be less impactful than that for in vivo testing.

For the design of this prototype the following assumptions were made:

- The "patient" had a weight of 70 kg.
- The insert would be assessed on the forces generated during walking and movements.
- If the insert became thinner than 6 mm, the stresses in the insert would increase exponentially. This means that the insert should be replaced to prevent further damage [13].

Several requirements were made for the design of the prototype:

- The insert had a minimum thickness of 8 mm [14].
- The insert had a maximum thickness of 16

mm [13].
- The insert would be able to measure linear penetration wear over a range of 0 to 2 mm.
- There would be separate wear measuring sensors on the lateral and medial sides.

Wishes for the insert were:
- The wear sensors had an accuracy of 0.02 mm. This accuracy was based on the minimum linear wear rate per year, as measured by Price [59].
- The insert could later on be used in vivo.
- The insert could measure the linear wear rate of the insert on the top and the bottom.

Design of insert

In SolidWorks, a model of the insert was created. The sizes and geometry of the model were based on the insert of a Sawbones knee with an implant. In this way, the available femoral part with an XS size fitted perfectly.

Position of wear sensors

The first step to determine the positions of wear sensors was to determine the locations where the highest forces acted on the insert. These areas would be favorable for wear sensors, since theoretically the largest amount of wear would be present in these areas of the insert. To determine these areas, a resistance sensor film was used in a test setup.

Resistance sensor film
A sensor film with resistance sensors was used to measure the force that the insert experienced during a knee movement. The sensor film contained resistance sensors that were connected with silver tracks and was produced by Holst. The film was made of polyethylene naphthalate (PEN)-foil and had a thickness of 175 µm. The sensors had a diameter of 6 mm and the distance from the midpoint to midpoint was 10 mm. The sensors worked in such a way that the lower the output, the higher the force that acted on the sensor. If the resistance was infinite, there would be no force acting on the sensor. To determine the ideal position of the wear sensors, resistance values from different sensors were measured to find out which sensor gave the lowest output. Since the sensors were quite large, four positions of the sensor film were chosen to cover the whole area of the insert. The positions of the wear sensors for different tests are shown in Figure 9. To confirm the stability of the results, the movement of the knee was repeated five times for each sensor at each position. 24 sensors were used for the determination of the area.

Test setup and position wear sensor
Figure 10 shows the test setup that was built to simulate the knee movement. For the tests, a tensile testing machine (Lloyd Instruments LS100K Plus) with a 5K load cell was used. A threaded end of M12 connected the load cell with a clevis. The clevis was used to simulate the hinge movement of the knee.

A connection piece was made by milling to connect the femoral component of the knee implant with the clevis. Since the female screw thread of the femoral component was angled, a male screw was used on the connection piece with an angle of 6^0. The technical drawing of this connection piece can be found in Appendix A. The simplification of eliminating the angle assured that the test setup was straight, and the tensile testing machine could be used for this test.

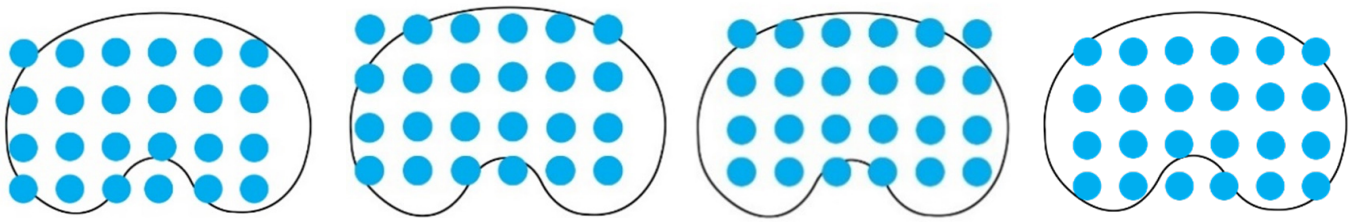

Figure 9 – Layout of the sensor positions for different trials. From left to right, trial 1 to trial 4.

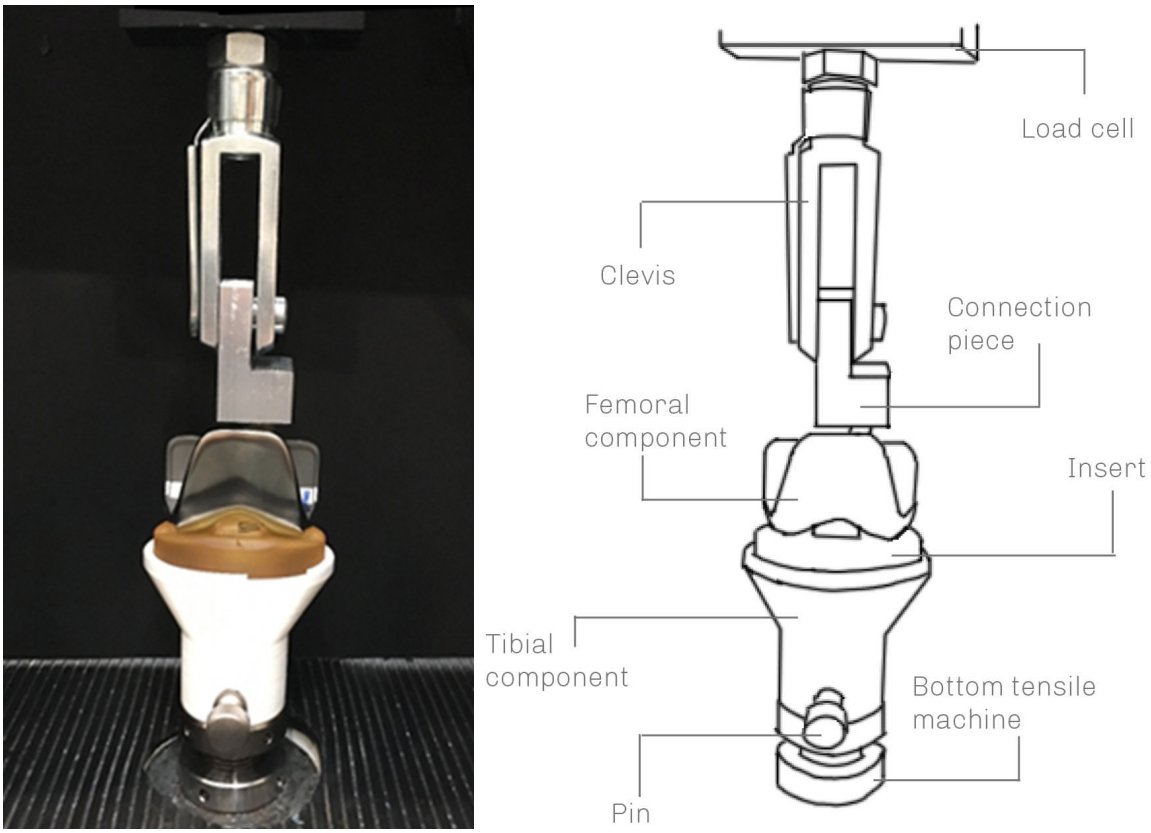

Figure 10 – Overview of the test setup. Left is a photo of the set up. Right is a systematic overview of the test setup.

The connection piece had a hole where it was attached to the clevis.

The femoral component was realized by a real femoral component of a left knee with a size of XS, produced by an unknown manufacturer.

The tibial part of the test setup was simulated by a 3D printed part. This component had a negative cutout of the insert, so the insert fitted nicely. The tibial component was fixed with a pin to the bottom of the tensile testing machine. Different tibial components were designed to fix the sensor film at different positions. This was done by making a slot through the part, in such a way that the sensor film fitted perfectly in it. The technical drawings of the tibial component can be found in Appendix B. In this way, the resistance sensors were placed under the insert on top of the tibial component. Different sensors were connected with different output wires. This means that every sensor had to be measured individually and read out with a multimeter (Figure 11).

The high E-modulus of the material that is usually used for knee insert, PE (±800 MPa) or similar material, makes the insert very stiff. Due to this stiffness, the resistance sensors did not give any output. Therefore, a foam model of the insert was chosen. This model made of foam rubber had the same measurements as the previous described insert that was created in SolidWorks.

Movement of the knee

Since no mechanical knee setup was available, several assumptions for the test setup were made. One of them, as explained earlier, was the choice to simulate the knee movement straight and not at an angle of 6^0. Choice was made to simulate the knee movement as a hinge movement. This that the knee setup was

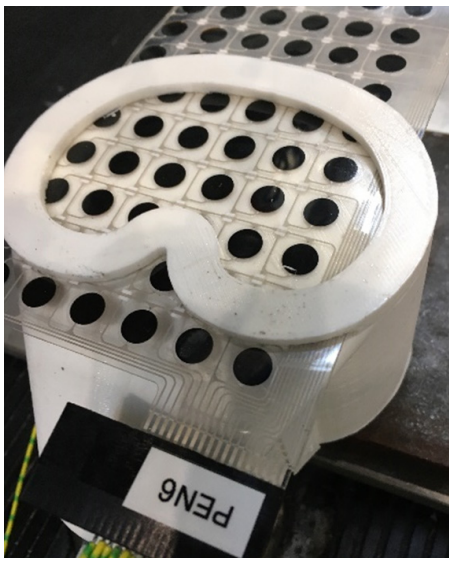

Figure 11 – Photo of the position of the sensors and the connection point.

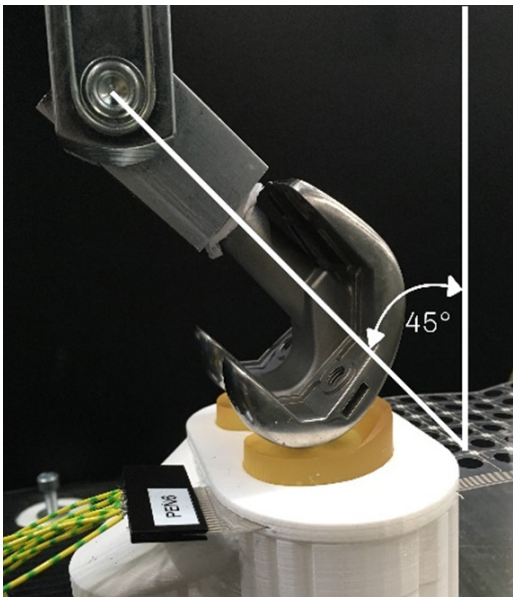

Figure 12 – Knee movement of the test setup. The photo displays the starting point.

only able to rotate and that only the rotating movement of the knee could be simulated. To create wear, the largest angle must be created with the femoral component. In this way, the contact area of the insert and the femoral component would be as large as possible. Since the femoral component had the limitation to rotate only but not translate, the knee movement was restricted from 45^0 to 57^0, as can be seen in Figure 12. After 57^0, it was physically not possible to move the knee without translating first, since the protuberance of the insert would stop the femoral part from getting to the front.

Wear prototype building process

To manufacture the wear measuring prototype, several steps were taken. First, cutouts for wear measuring tracks in the CAD model were made. The first cutout was positioned at 0.6 mm from the top and had a thickness of 0.1 mm. The second cutout was positioned at 0.6 mm below the first cutout and the third 0.6 mm below the second. The cutouts were positioned at the same heights on the lateral side and on the femoral side of the insert. The width of the tracks i.e., the cutouts, was 0.65 mm. The cutouts covered as much as area as possible, without interconnecting with each other, otherwise there would be no accurate results of the whole track area. The two ends of each track had to be accessible in order to be able to get to the tracks. To have better access to the end of the tracks, a bit of the layers above the track was removed, so from the side it looks like a stair. The heights of the tracks were chosen in such a way that the separately printed parts would be handleable. If the layers became too thin, they would break easily, and no prototype could be made.

The CAD model was sliced in the number of tracks plus 1 and in such a way that all the cutouts were accessible from the top. Different parts of the insert were 3D printed on a Formlabs Form 2 printer with the Formlabs Form 2 clear resin. Then, the cutouts of the tracks were filled with silver electron paint (VFP Ink Technologies). This paint was able to create a conductive track. Afterwards, the tracks were cured by a JBC TE500 Advanced heating element to dry the tracks and keep the conductivity optimal. Every track was checked with a multimeter on its conductivity at random positions to ensure that the tracks did not have unwanted interconnections. The technical drawing of the slices can be found in Appendix C.

After the conductivity check, the layers were glued to each other with Araldite 2000+. The layers had to be put together carefully, since any movement could increase the possibility that the silver tracks would stick to the glue at the wrong place and became destroyed.

Test setup to create wear

The evaluation of the prototype was performed in the following way. The same tensile testing machine, components of the test setup and knee movement were used. To speed up the wear process, sand paper with 60 grit was adhered with double-sided tape to the femoral part, as can be seen in Figure 13. In this way, the time-consuming wear test could be finished in less cycles and the prototype could be evaluated sooner. Since the wear of the implant still took a lot of cycles, the sand paper was changed every 1,500 cycles, or when it became unattached in

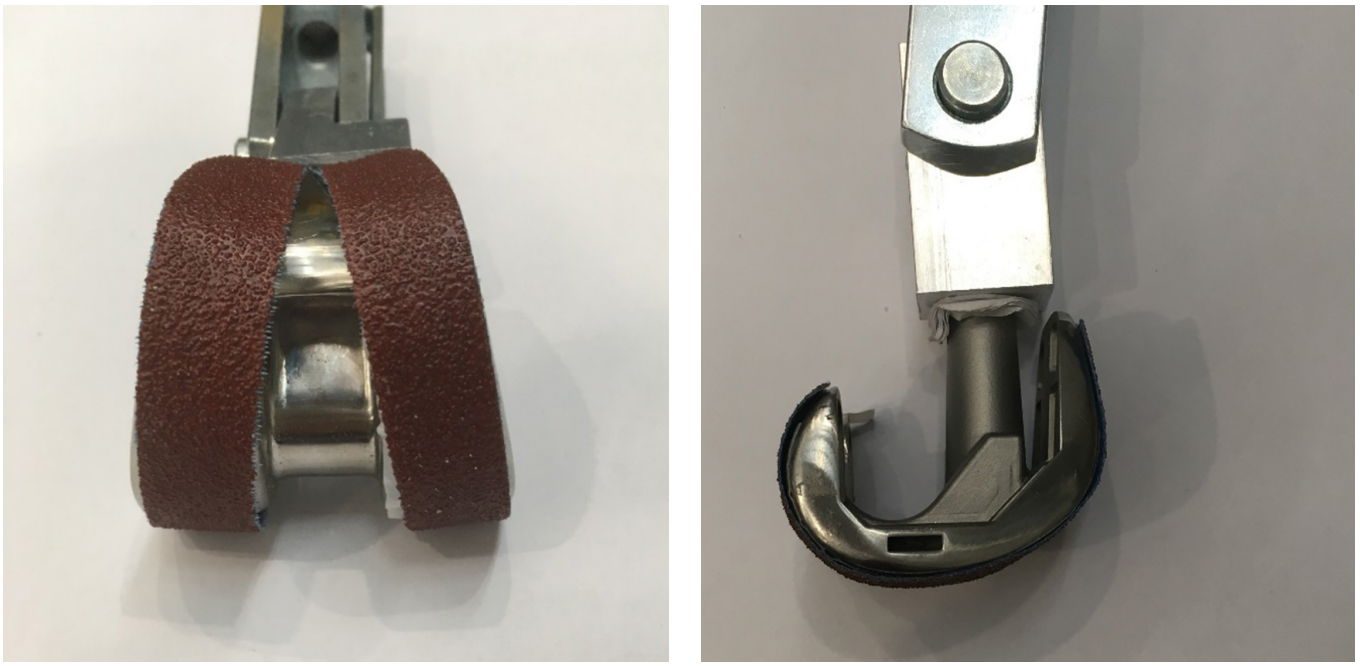

Figure 13 – Photo of the femoral head covered with sand paper. Left photo is the view from the front, and the right photo is the view from the side.

order to give an optimal result.

To assure that the track would wear down at the pre-determined height, the resistance of the tracks was checked if it became infinite. At this point, the depth of the wear was measured with a caliper and compared with the height of the track. This was done for all the tracks in one prototype.

RESULTS

Resistance sensors

When no force was acting on the resistance sensor, the output would be infinite. Some of the sensors only gave this infinite output and the results were therefore not worth showing. The graphs of the sensors that gave at a point outputs other than infinite, are given in Appendix D. Due to the limitations in Excel, an infinite output was noted as 1.00x1059. In the graphs these measuring points are not shown, since it will distort the graph when the measuring points that give an output other than infinite are more interesting. The graphs are divided into the four sections of the different tests with different sensor positions, as described in the Materials and Methods chapter.

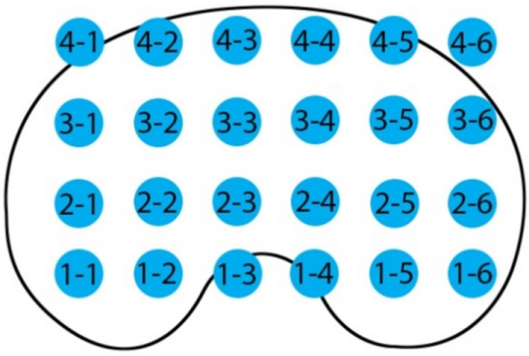

Figure 14 – Overview of the sensor numbering.

To differentiate the sensors, codes were assigned. The first number of the code is the row of the sensor, counted from the bottom, and the second number is the number of the sensor counted from the left. For example, sensor 2-6 is the sensor that is on the second row from the bottom and on the right side. The overview of the sensor numbers can be found in Figure 14.

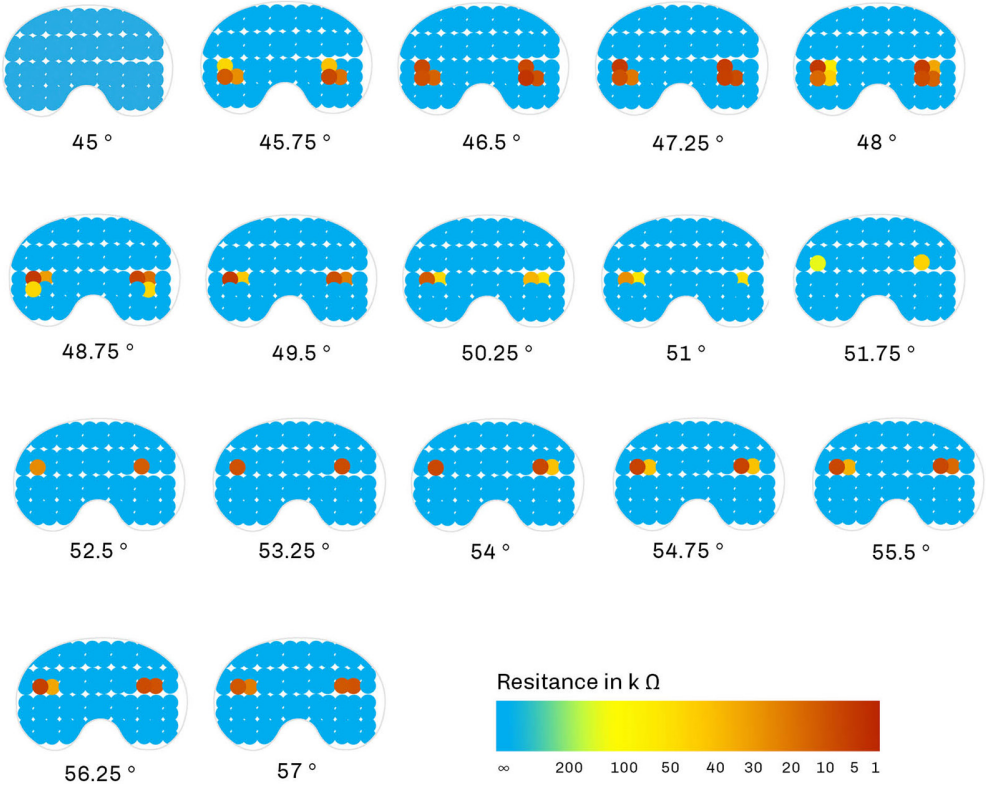

Figure 15 – Heat maps of the outputs of the resistance sensors. The outputs of every 0.75° of the knee movement are shown. In the legend the conversion of the color to kΩ can be found.

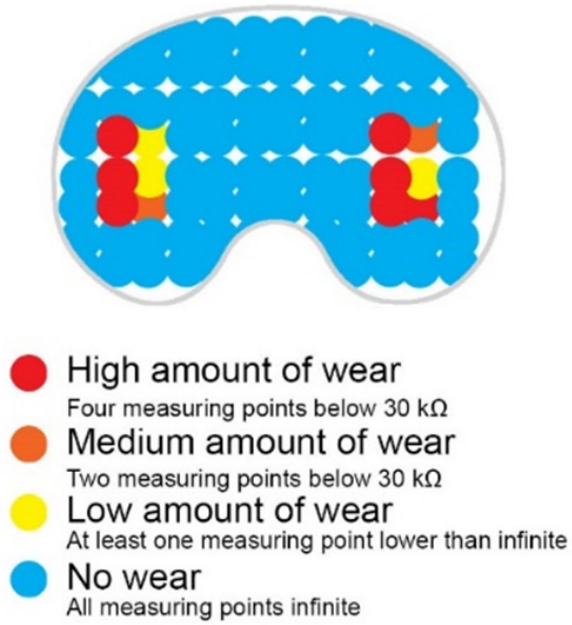

Figure 16 – Combined heatmap of the expected wear distribution of the insert.

Since the data of the separate sensors gave a better view when it was put altogether, heatmaps of every 0.75^0 were created, as shown in Figure 15. For the output of the sensors, the average number of 5 trials was taken. At 45°, no resistance was measured since the tensile machine was in its neutral position. The maximum values were combined in a total image of the areas that would be affected by the femoral component. Based on the colors, the locations where the highest amount of wear that would take place could be identified. These were combined in the heat map, as shown in Figure 16. The amount of wear was based on the number of measuring points where a certain resistance was measured.

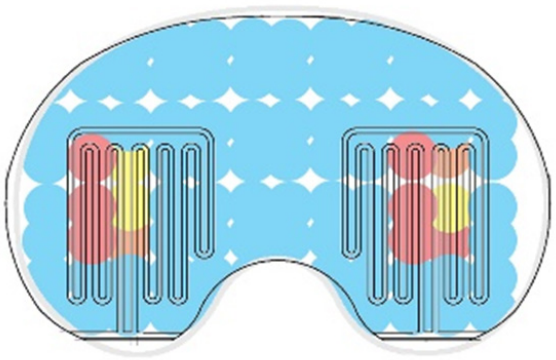

Figure 17 – Positions of the wear sensors in the insert. View from the top.

Based on these wear visualizations, the positions of the wear sensors were chosen, as shown in Figure 17.

Prototype

The resulting prototype had three layers of conductive tracks on the medial and lateral sides, making it have six wear sensors in total. The measurements of the prototype are defined in the technical drawing of the assembly in Appendix E and are the same as the previously described insert in the section of Materials & Methods. Different slices of the prototype can be seen in Figure 18. The thickness of the assembled insert was 9.35 mm. The resistance of all silver tracks could be measured with a multimeter. The overall overview of the assembly is shown in Figure 19.

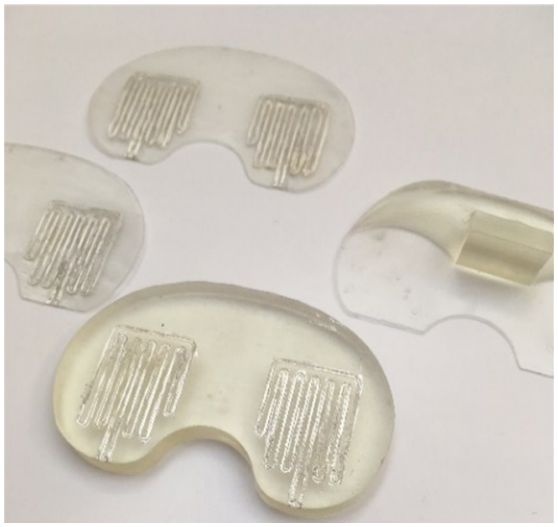

Figure 18 - Different slices of the prototype

Figure 19 - Assembled prototype

Evaluation of prototype

The insert was tested in the wear test setup, as described in the previous chapter. To give a better overview of the results, the tracks were numbered. The highest track on the medial side is number 1, on the lateral side number 2, the second highest track on the medial side is number 3 and so on. An overview of this numbering can be found in Figure 20. This makes the odd numbers the tracks on the medial side and the even numbers the tracks on the lateral side. In Table 1, the resistance of the track, the number of cycles it took to change its resistance to infinite and the depth of the wear when the resistance turned to infinite are given.

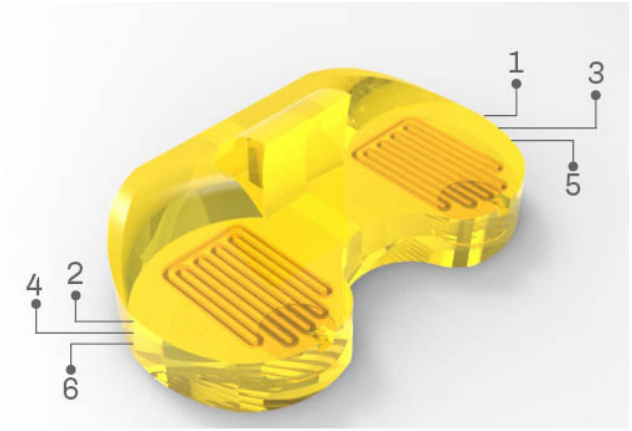

Figure 20 – Numbering of tracks.

In Figures 21-26, the photos of the insert after these cycles are presented. However, since these are 2D photos, it is not very clear which areas are worn down. To make wear visible, wear patterns per layer are contoured.

Track number	Defined track depth	Resistance begin test	Cycles when resistance infinite	Wear depth
Track 1	0.6 mm	40.3 Ω	6732	0.65 mm
Track 2	0.6 mm	69.7 Ω	9974	0.65mm
Track 3	1.2 mm	38.9 Ω	14384	1.35 mm
Track 4	1.2 mm	128.4 Ω	20413	1.35 mm
Track 5	1.8 mm	76.3 Ω	23928	2.15 mm
Track 6	1.8 mm	92.3 Ω	32050	2.15 mm

Table 1 – Overview of the amount of resistance, the number of cycles needed to wear the sensor down and the measured wear depth.

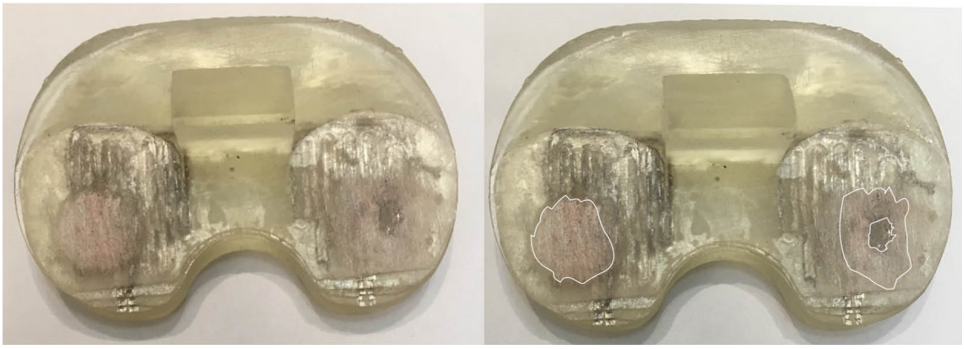

Figure 21 – Photo of insert when the first track on the right (medial side) wore through. The white lines on the right contour the wear of the different layers.

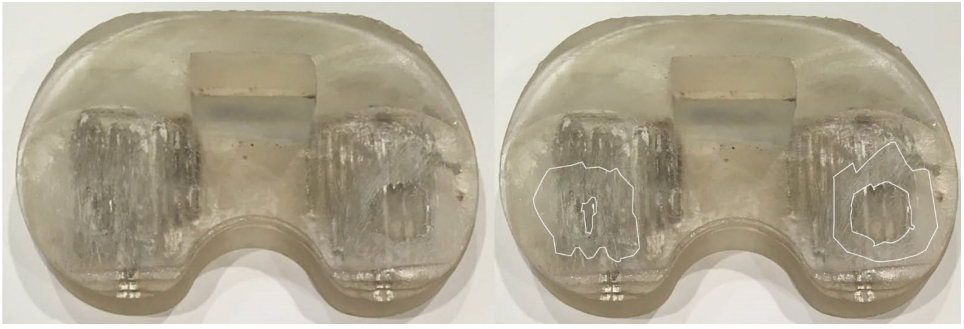

Figure 22 - Photo of insert when the second track on the right (medial side) wore through. The white lines on the right contour the wear of the different layers.

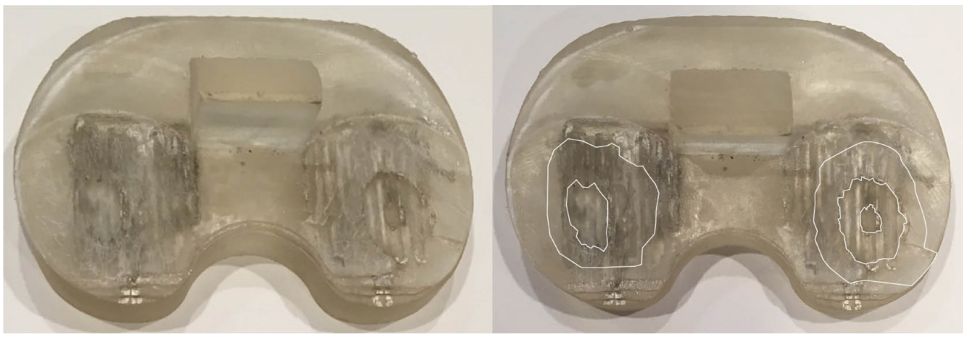

Figure 23 - Photo of insert when the first track on the left (lateral side) wore through. The white lines on the right contour the wear of the different layers.

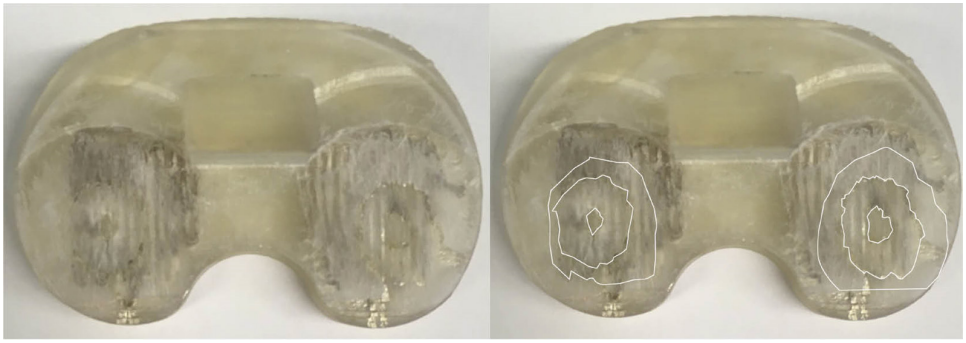

Figure 24 - Photo of insert when the second track on the left (lateral side) wore through. The white lines on the right contour the wear of the different layers.

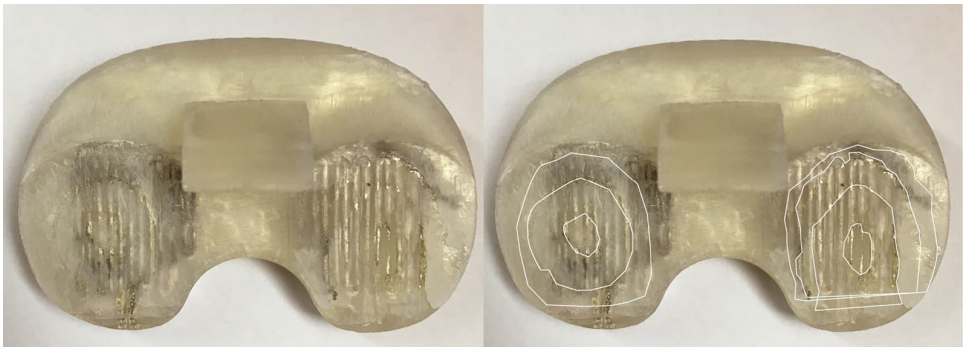

Figure 25 - Photo of insert when the third track on the right (medial side) wore through. The white lines on the right contour the wear of the different layers.

Figure 26 - Photo of insert when the third track on the left (lateral side) wore through. The white lines on the right contour the wear of the different layers.

During each 1,500 cycles of test, the load differed a bit. In Figure 27, loads at different cycle numbers can be seen. The frequency of the movement was 0.5 Hz. The load in the second cycle had a maximum of 859.82 N (1.25 xBW) and then stabilized to about 660 N (0.96 xBW). A small decrease in load at about 990 cycles was the point where the tape on sandpaper got loose but stuck again at 1,050 cycles.

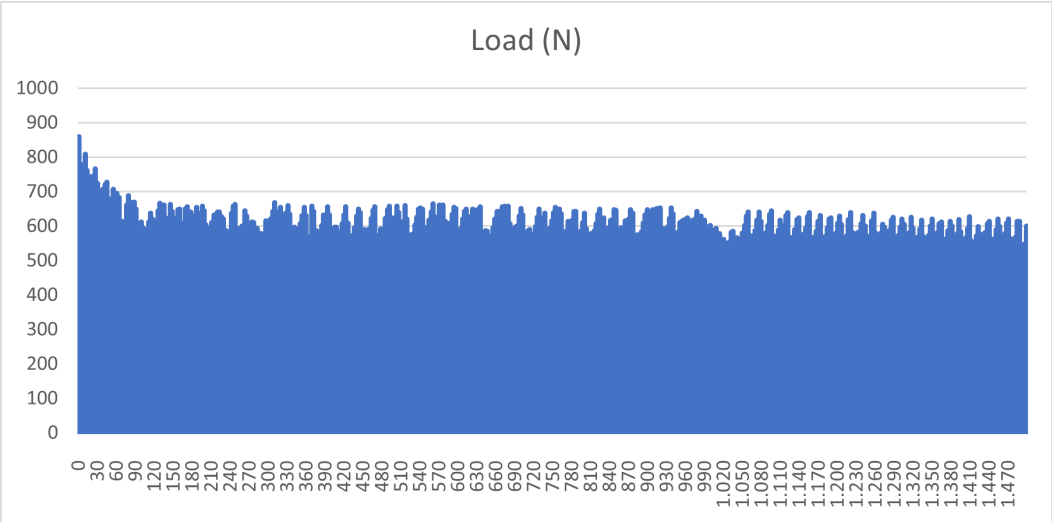

Figure 27 – Graph of the applied load by the tensile testing machine for every cycle.

DISCUSSION

Knee movement

For the test setup, the movement of the knee was simulated like a hinge. The hinge was positioned quite high above the femoral part, due to the physical restrictions in the test setup. A human knee joint has six degrees of freedom and obviously a hinge is quite simplistic. It is really hard to simulate the knee joint in a straightforward mechanical way without the use of complex test setups. There are several knee test setups that are able to simulate the knee movement in a more realistic way, although these were not accessible in this project. With such complex test setups, McGloughlin and Kavanah concluded that a higher sliding-rolling ratio led to a higher wear rate [64].

In the present research, the varus-valgus alignment was chosen at 0° to make the test setup more feasible. However, in reality, the femoral component is made for a varus of 6° and this is far more realistic than 0^0, since the patient at with a bone alignment of 0° will have serious O-legs.

Resistance sensors

The resistances of some of the sensors differed quite a lot. For example, the resistance distribution of sensor 2-1 in test 4 differed over a range from 40 kΩ to 102 kΩ. The high resistances are a sign that the sensor is pushed only slightly. The differences in resistance were probably because the femoral head in one trial was at a more favorable position than that in the other trial, because the test setup had a little mechanical clearance.

As shown in the heatmaps, the resistance distribution on the medial side was quite the same as that on the lateral side. However, two sensors registered a bit more resistance on the medial side than on the lateral side. As shown in the study of Plante-Bordeneuve, this could be because the alignment of the test setup was at 0°, while a neutral position of the knee is normally about 6° [47]. The varus position will lead to more medial wear.

The sensors used in this study were quite large, 6 mm in diameter. Despite the efforts to get the whole insert surface area covered, the results “within” each sensor were not very accurate. It could be possible that only half of the sensor experienced a force, which would lead to a significant change in resistance. However, this could not be read from the measurements.

Prototype

The resistances of some of the sensors differed quite a lot. For example, the resistance distribution of sensor 2-1 in test 4 differed over a range from 40 kΩ to 102 kΩ. The high resistances are a sign that the sensor is pushed only slightly. The differences in resistance were probably because the femoral head in one trial was at a more favorable position than that in the other trial, because the test setup had a little

The cycles that were needed to wear the insert down differed between the medial side and the lateral side of the insert. The number of cycles that was needed to break the track can be seen in the Table 2. The medial side, i.e., the odd track numbers, wore down more easily than the lateral side. In the heat maps, the medial side appeared

Track number	Number of cycles from previous track needed to wear down
Track 1	6732
Track 2	9974
Track 3	7654
Track 4	10439
Track 5	9544
Track 6	12637

Table 2 – Number of cycles to wear each track down.

to experience somewhat more force than the lateral side. Since the forces are correlated to wear, the medial part wore down sooner than the lateral part. As explained earlier, this is probably due to the alignment of the test setup.

The numbers of cycles that were needed for the tracks to wear down were different. This could be explained in different ways. First, the femoral head needed extra space to "get down". Otherwise it would not get to the depth of the tracks. Since the femoral part had to wear down more volume of the insert, it would take longer to get to a next layer. Moreover, the movement of the knee was based on an unworn insert. This means the area of contact would reduce as the insert wore down.

The wear measuring sensors had first resistance values in a range from 40.3 Ω to 128.4 Ω. When the tracks were worn down, the resistance would change almost immediately to infinite. The wear per cycle was apparently enough to destroy the track in one movement. Because sandpaper was used for the test setup, the wear was accelerated a lot. This means that with the tests without the sandpaper the change in resistance should be visible during the wearing of the tracks. Every time the femoral head will wear the track a bit down, the resistance will increase. Eventually, when there is nothing left at a certain point, the resistance will change to infinite. Unfortunately, this transition was not visible with the used test setup due to the high speed of the wear.

After each 1,500 cycles of the knee movement, the insert was cleaned. This was done to check the progress of the wear. This could have an influence on the wear pattern. Since residual particles were removed, they would not influence the wear anymore in further cycles of the test. However, in the in vivo situation, wear debris will not disappear and will stay between the femoral head and the knee insert. This would influence the contact surface (three-body abrasive wear) and therefore the speed of wear.

This prototype was made of Form 2 clear resin. This photopolymer is specially made for 3D printing on a Formlabs 3D printer and is not produced for implants. This means the material is not biocompatible and has not the same mechanical properties, as e.g., UHMWPE. The mechanical properties of this material surely influenced the speed of wear, because Form 2 clear resin wears down far more easily than a material especially selected for the knee implant insert (i.e., UHMWPE). Currently, some research group are studying the various possibilities to 3D printed implants with different biocompatible materials [65], [66].

The calliper has an accuracy of 0.05 mm. It is not the most accurate tool to match the accuracy of the resistance sensors. However, unfortunately, this was the only tool available and should therefore be used.

At one point, a bigger part of the insert broke as can be seen in the difference between Figure 22 and 23. It was the part of the insert right below that would experience no forces, according to the heat maps. An explanation for the breakage of this part could be the use of not well distributed glue. The layer was glued on the previous layer and should be adhered well. However, apparently, not the whole layer got the same amount of glue. This part probably had no glue on it, and since its "connecting" material wore down, the part broke off.

An important part of the evaluation of the prototype was of course the accuracy of the wear sensors. As can be seen Table 3, the wear of the insert was not the same as the pre-determined heights of the sensors. The deeper

Track number	Interval pre-defined track depth	Interval wear depth
Track 1	0.6 mm	0.65 mm
Track 2	0.6 mm	0.65 mm
Track 3	0.6 mm	0.70 mm
Track 4	0.6 mm	0.70 mm
Track 5	0.6 mm	0.70 mm
Track 6	0.6 mm	0.70 mm

Table 3 – Interval of the tracks and interval of the wear depth

the tracks were placed, the less accurate the pre-determined and the measured depth was. This was of course due to the inaccuracies of the previous layers. If the inter-layers were taken into consideration, it would be clearer. The overall accuracy of the sensors can be calculated by dividing the total predefined track depth by the total of the intervals of the wear depths. This will result in that the resistance sensors have an accuracy of 88% in this prototype. A reason for this relatively low accuracy can be the glue layers that were placed between the layers of the insert. These glue layers added their amounts to the thickness. Since the overall thickness of the prototype was 9.55 mm, but not 9.30 mm, as pre-determined in the technical drawings, the source of the reduction of the accuracy became clear.

Only three layers of tracks were used in the prototype. This means the linear wear rate could be measured over a depth of 0.6 mm. This is not the depth expected at the beginning of the present study. When using the Lepus NextGen 3D printer, it is possible to print the tracks while printing the prototype. This would make the silver tracks be positioned far more accurately in the prototype. By using a 3D printer for creating the whole part in one time, instead of creating a prototype of different layers, the layer thickness will be less important and can go lower than in the case that the different layers are printed separately. In addition, the glue used to adhere the parts to each other also influenced the thickness of the total part. A risk of using the glue is that it can easily destroy the silver tracks. To avoid this risk and improve the accuracy, it is recommended to print the insert in one time on a 3D printer.

In this prototype, the wear can be measured at six points: three points on the medial side and another three points on the lateral side. By increasing the number of tracks, it should be possible to measure the wear at more depths and in more areas.

The current prototype could measure the wear of the insert after the wear depth reached 0.65 mm. Taking into consideration the average of the wear rate of a knee insert (0.12 mm/year), it will take about 5,5 years to be able to measure the first signs of wear. In the most favorable scenario (wear rate: 0.021 mm/year [59]), it will even take about 30 years to be able to measure the first signs of wear. Since most of the knee insert will only last 15 years in the body, the insert with wear sensors will be quite unrealistic. For this reason, it is recommended to integrate wear sensors into the insert closer to the surface. By producing the insert with embedded wear sensors by means of a Lepus NextGen printer, it will be possible to achieve a layer thickness of 50 µm. This will make it possible to indeed create an insert with sensors that are closer to the surface.

Furthermore, was this prototype not able to measure the linear wear on the top and the bottom. This was stated in one of the wishes, because of several researches that showed that there occurs also wear at the bottom of the insert [67], [68]. However, due to the simplified test setup there did not occur any movement at the bottom of the insert and was the placement of the wear sensors in the bottom out of the scope of this project.

For this prototype silver paint was used for creating the tracks. However, the paint is not biocompatible and can therefore not be used in an in vivo design. Since the insert will wear down

over time, it should be safe to choose a material that does not need coating. Another material that is biocompatible, conductive and can be 3D printed should be chosen.

A point of attention is that since most of the femoral components are made of CoCr-based alloys or titanium, the femoral part is electrically conductive. This can have an influence on the output of the integrated wear sensors. Since the wear measurement is based on the resistance, it is possible that a track has worn down, but the femoral component fits in such a way on it that the resistance is not infinite. Since in the wear tests sandpaper was attached to the femoral head, this was not the case. However, the femoral head moves over a larger surface area of the insert and therefore will not always be the "conductive connection" between broken tracks.

The measurements of the insert were mostly based on the measurements of the insert of the Sawbones Clear knee implant. The organic forms were all simplified, which resulted in a quite flat top of the insert. This made measuring the wear rate with a caliper easier. However, in inserts that are used in vivo, the surfaces of the inserts are not flat. This should be considered in follow-up research.

This study did not take the creep of the insert in consideration. The creep could appear due to the tibiofemoral forces that the insert is exposed to. Using micro-CT as an in vivo wear measuring method, it is difficult to distinguish the actual wear amount from creep. Since in the studied concept the wear tracks are integrated in the insert, there will be a clear difference between the creep and wear. The tracks will only break due to wear, so if the resistance changes to infinite, it is caused by the wear without doubt.

It is important to mention is that the results obtained from the present tests of the insert, cannot be compared with the wear of a healthy knee. The insert has mechanical properties other than a meniscus. In this research, some simplifications in the knee movement to increase the feasibility of the project were made. Even when in vivo studies will be performed with the sensor-integrated inserts, the results of such insert cannot be extrapolated to a healthy knee. This is because the patient who gets TKR including a knee insert, most likely suffers from OA. It means that he/she may have an adjusted gait due to previous pain and the insert will experience higher peak forces [69]–[71].

Comparing the heat maps with the photos of the worn-down insert, some similarities can be found. The position of the wear is indeed almost the same and the surface areas are the same as those that are expected to wear down earlier. However, the wear sensors themselves could not demonstrate these agreements. This is due to the inaccuracy of the wear sensors. If wear sensors are positioned closer each other, they may show the wear pattern better.

The question rises as to if more wear sensors in one knee insert are needed, or if one sensor only at a certain height can fulfill its function. The choice of the number of wear sensors can be based on several considerations. It is important to consider the primary function of wear sensors: will they be in the insert to provide information as to when the insert should be replaced, or will they be in the insert to provide information about the wear pattern and improve the rehabilitation of the patient. For the first function, it is indeed possible to embed a wear sensor in the insert at a certain height. When the sensor is broken, the physician will be alarmed, and the patient may need to have a revision surgery. However, when the integrated wear sensors are intended for the second function, more wear sensors are needed to provide precise information about the wear of the insert as soon as possible. In this situation, it is for example possible to modify the gait of the patient in order to have more consistent wear at the medial and lateral parts of the insert. Or the wear pattern can be used to improve the alignment of the insert in the future.

CONCLUSION

The main objective of the current study was to develop and evaluate an insert with integrated wear sensors that could eventually be used in vivo. To achieve this objective, first the position of the wear sensors was determined by using resistance sensors. These resistance sensors showed that there would be a bit more wear on the medial side than on the lateral side. This was later on confirmed by the wear test. Then, a prototype was created that had three layers of conductive tracks. By measuring the resistance in the tracks, the wear of the tracks could be measured. The results from the evaluation proved the concept and showed that wear sensors at different heights worked well. However, this prototype was inaccurate due to the glued layers. Therefore, it is important to improve the method to fabricate a more accurate prototype as one single piece. Thereby did the test setup had its limitations due to the simplifications that were made.

The prototype created in this research cannot be used in vivo. The materials used for inserts and tracks should be changed to be biocompatible ones. Furthermore, the way of transferring data should be considered.

Further steps should be taken to realize the insert in such a way that it can be used in vivo. Despite this, the research reported in this thesis demonstrates that conductive tracks at different heights of the insert can be a feasible solution to measuring wear and the concept can be used eventually in vivo.

RECOMMENDATIONS FOR FUTURE WORK

Having performed proof of concept tests of the wear-measuring sensors, several recommendations can be made to improve this technique.

The first recommendation will be to create the complete insert on a 3D printer. This will increase its accuracy, since the adhesive between the layers does not have to be taken into consideration any more. This can be combined easily with another recommendation: an increment in track number. An increment in track number can create the possibility to analyze the wear pattern in a more accurate way, since tracks will be closer to each other.

One may also look at the possibilities to add more tracks to each layer. In this research, differentiation between the medial side and lateral side was made. With more tracks, one can differentiate the front side and back side of the insert and even make distinction within the medial and lateral parts. The choices of the number and positions of wear sensors can be based on, for example, retrieved implants.

Unfortunately, it was not possible in this study to create an insert that could be used in vivo. Before that can be created, several steps have to be taken into consideration, such as the choice of materials and the data transmitting technique. The material of the insert as the wear tracks should be biocompatible. This is quite easy for the insert itself, since several materials that are suited and used for knee inserts are already on the market. In making material choice, it is important to consider the material that can be 3D printed. Since there are currently a number of manufacturers that create customized 3D printed knee implants, there must be a material available that can fulfill these requirements. Choosing a material for the conductive tracks will, however, be somewhat harder. Conductive materials such as titanium and CoCr-alloys are currently used for implants. There are possibilities to 3D print these materials, but 3D printing is mostly done with another technique, namely selective laser melting. Combining 3D printing these materials with, for example PE, will be very cumbersome. In that case one may discuss if 3D printing the insert is the most favorable production technique. Conductive polymers like polyaniline are another option for the material of the tracks. At present, a lot of research on the 3D printability of these kind of polymers is being performed [72]–[74].

The output of the wear sensors should be received and displayed. If the insert is placed in the body, there is no option to use a multimeter. Therefore, one must think about a solution for this data transmission. One option is to integrate a small printed circuit board into the insert that can read out the signals and transmit them via a wireless connection such as Bluetooth or Near-field communication (NFC). However, integrating electronics into the insert must be done carefully since the electronics have to be protected and can never be in touch with human tissue. Therefore, a passive system will be favorable. One may consider using magnetism or similar techniques that can be measured near the body without the use of electronics inside the body.

ACKNOWLEDGEMENTS

I wish to thank various people for their contribution to this project; Mr. Reese and Mr. Bruning, staff of TNO, for their valuable and constructive suggestions during the development of the research work, Mr. Maalderink and Ms Burghoorn, also staff of TNO, for providing me several parts for the prototypes. My grateful thanks are also extended to Mr. Leeflang for his help in thinking through the test setup and help in performing the mechanical tests at the TU Delft. Special thanks should be given to Dr. Zhou, my graduation project supervisor for his guidance, valuable support and accurate comments. Finally, I want to thank TNO for the opportunity to realize my graduation project in this company.

REFERENCES

[1] Landerlijke Registratie Orthopedische Implantaten, "LROI - Annual Report 2017," no. June, p. 184, 2017.

[2] A. J. R. Registery, "AJRR Annual Report 2016," 2016.

[3] P. Porter, M. Borroff, P. Gregg, A. MacGregor, and K. Tucker, "10th Annual Report 2013 National Joint Registry for England, Wales and Northern Ireland," *Natl. Jt. Regist.*, 2013.

[4] J. A. Roman-Blas, S. Castañeda, R. Largo, and G. Herrero-Beaumont, "Osteoarthritis associated with estrogen deficiency," *Arthritis Res. Ther.*, vol. 11, no. 5, pp. 1–14, 2009.

[5] D. D. D'Lima, B. J. Fregly, S. Patil, N. Steklov, and C. W. Colwell, "Knee joint forces : prediction , measurement , and significance," *Proc. Inst. Mech. Eng. H.*, vol. 226, no. 2, pp. 95–102, 2013.

[6] J. A. Singh and D. G. Lewallen, "Time Trends in the Characteristics of Patients Undergoing Primary Total Knee Arthroplasty," *Arthritis Care Res. (Hoboken).*, vol. 66, no. 6, pp. 897–906, 2014.

[7] D. K. Bae, S. Do Cho, S. K. Im, and S. J. Song, "Comparison of Midterm Clinical and Radiographic Results Between Total Knee Arthroplasties Using Medial Pivot and Posterior-Stabilized Prosthesis—A Matched Pair Analysis," *J. Arthroplasty*, vol. 31, no. 2, pp. 419–424, Feb. 2016.

[8] J. Fisher et al., "A novel method for the prediction of functional biological activity of polyethylene wear debris," *Proc Inst Mech Eng H*, vol. 215, no. 2, pp. 127–132, 2001.

[9] P. F. Sharkey, P. M. Lichstein, C. Shen, A. T. Tokarski, and J. Parvizi, "Why are total knee arthroplasties failing today-has anything changed after 10 years?," *J. Arthroplasty*, vol. 29, no. 9, pp. 1774–1778, 2013.

[10] C. A. Engh, R. L. Zimmerman, R. H. Hopper, and G. A. Engh, "Can Microcomputed Tomography Measure Retrieved Polyethylene Wear? Comparing Fixed-bearing and Rotating-platform Knees," *Clin. Orthop. Relat. Res.*, vol. 471, no. 1, pp. 86–93, Jan. 2013.

[11] M. S. Kuster and G. W. Stachowiak, "Factors Affecting Polyethylene Wear in Total Knee Arthroplasty," *Orthopedics*, vol. 25, pp. S235–S242, 2002.

[12] R. A. Cooper, C. M. McAllister, L. S. Borden, and T. W. Bauer, "Polyethylene debris-induced osteolysis and loosening in uncemented total hip arthroplasty. A cause of late failure," *J. Arthroplasty*, vol. 7, no. 3, pp. 285–290, 1992.

[13] D. Bartel, V. Bicknell, M. Ithaca, and T. Wright, "The Effect of Conformity, Thickness, and Material on Stresses in Ultra-High Molecular Weight Components for Total Joint Replacement," in *Classic Papers in Orthopaedics*, London: Springer London, 2014, pp. 93–96.

[14] J. P. Collier, M. B. Mayor, J. L. McNamara, V. A. Surprenant, and R. E. Jensen, "Analysis of the Failure of 122 Polyethylene Inserts From Uncemented Tibial Knee Components," *Clin. Orthop. Relat. Res.*, vol. 273, pp. 232–242, 1991.

[15] D. D. D'Lima, S. Patil, N. Steklov, S. Chien, and C. W. Colwell, "In vivo knee moments and shear after total knee arthroplasty," *J. Biomech.*, vol. 40, no. SUPPL. 1, 2007.

[16] D. D. D'Lima, S. Patil, N. Steklov, J. E. Slamin, and C. W. Colwell, "In vivo knee forces after total knee arthroplasty," *Clin. Orthop. Relat. Res.*, no. 440, pp. 45–49, 2005.

[17] B. J. Fregly et al., "Grand challenge competition to predict in vivo knee loads," *J. Orthop. Res.*, vol. 30, no. 4, pp. 503–513, 2012.

[18] M. L. Harris, P. Morberg, W. J. M. Bruce, and W. R. Walsh, "An improved method for measuring

tibiofemoral contact areas in total knee arthroplasty: A comparison of K-scan sensor and Fuji film," *J. Biomech.*, vol. 32, no. 9, pp. 951–958, 1999.
[19] B. J. Fregly, Y. Bei, and M. E. Sylvester, "Experimental evaluation of an elastic foundation model to predict contact pressures in knee replacements.," *J. Biomech.*, vol. 36, no. 11, pp. 1659–68, Nov. 2003.
[20] A. Arami et al., "Instrumented knee prosthesis for force and kinematics measurements," *IEEE Trans. Autom. Sci. Eng.*, vol. 10, no. 3, pp. 615–624, 2013.
[21] S. Matsuda, S. E. White, V. G. Williams, D. S. McCarthy, and L. a Whiteside, "Contact stress analysis in meniscal bearing total knee arthroplasty.," *J. Arthroplasty*, vol. 13, no. 6, pp. 699–706, 1998.
[22] C. Stukenborg-Colsman, S. Ostermeier, C. Hurschler, and C. J. Wirth, "Tibiofemoral contact stress after total knee arthroplasty," *Acta Orthop. Scand.*, vol. 73, no. 6, pp. 638–646, 2002.
[23] L. Mohanty, S. C. Tjin, D. T. T. Lie, S. E. C. Panganiban, and P. K. H. Chow, "Fiber grating sensor for pressure mapping during total knee arthroplasty," *Sensors Actuators, A Phys.*, vol. 135, no. 2, pp. 323–328, 2007.
[24] T. Wehner, L. Claes, and U. Simon, "Internal loads in the human tibia during gait," *Clin. Biomech.*, vol. 24, no. 3, pp. 299–302, 2009.
[25] C. R. Winby, D. G. Lloyd, T. F. Besier, and T. B. Kirk, "Muscle and external load contribution to knee joint contact loads during normal gait," *J. Biomech.*, vol. 42, no. 14, pp. 2294–2300, 2009.
[26] H. J. Kim, J. W. Fernandez, M. Akbarshahi, J. P. Walter, B. J. Fregly, and M. G. Pandy, "Evaluation of predicted knee-joint muscle forces during gait using an instrumented knee implant," *J. Orthop. Res.*, vol. 27, no. 10, pp. 1326–1331, 2009.
[27] Y. C. Lin, J. P. Walter, S. A. Banks, M. G. Pandy, and B. J. Fregly, "Simultaneous prediction of muscle and contact forces in the knee during gait," *J. Biomech.*, vol. 43, no. 5, pp. 945–952, 2010.
[28] S. J. G. Taylor, P. S. Walker, J. S. Perry, S. R. Cannon, and R. Woledge, "The forces in the distal femur and the knee during walking and other activities measured by telemetry," *J. Arthroplasty*, vol. 13, no. 4, pp. 428–435, 1998.
[29] D. D. D'Lima, S. Patil, N. Steklov, J. E. Slamin, and C. W. Colwell, "Tibial forces measured in vivo after total knee arthroplasty," *J. Arthroplasty*, vol. 21, no. 2, pp. 255–262, 2006.
[30] B. J. Zhao, D., Banks, S.A., D'Lima, D.D., Colwell Jr., C.W., Fregly, "In Vivo Medial and Lateral Tibial Loads during Dynamic and High Flexion Activities," *J. Orthop. Res.*, vol. 5, pp. 593–602, 2007.
[31] D. D. D'Lima, N. Steklov, S. Patil, and C. W. Colwell, "The Mark Coventry award: In vivo knee forces during recreation and exercise after knee arthroplasty," *Clin. Orthop. Relat. Res.*, vol. 466, no. 11, pp. 2605–2611, 2008.
[32] A. Mündermann, C. O. Dyrby, D. D. D'Lima, C. W. Colwell, and T. P. Andriacchi, "In vivo knee loading characteristics during activities of daily living as measured by an instrumented total knee replacement," *J. Orthop. Res.*, vol. 26, no. 9, pp. 1167–1172, 2008.
[33] B. J. Fregly, D. D. D'Lima, and C. W. Colwell, "Effective gait patterns for offloading the medial compartment of the knee," *J. Orthop. Res.*, vol. 27, no. 8, pp. 1016–1021, 2009.
[34] M. A. Wimmer and T. P. Andriacchi, "Tractive forces during rolling motion of the knee: Implications for wear in total knee replacement," *J. Biomech.*, vol. 30, no. 2, pp. 131–137, 1997.
[35] B. Heinlein et al., "ESB clinical biomechanics award 2008: Complete data of total knee replacement loading for level walking and stair climbing measured in vivo with a follow-up of 6-10 months," *Clin. Biomech.*, vol. 24, no. 4, pp. 315–326, 2009.
[36] J. C. Erhart, C. O. Dyrby, D. D. D'Lima, C. W. Colwell, and T. P. Andriacchi, "Changes in in vivo knee loading with a variable-stiffness intervention shoe correlate with changes in the knee adduction moment," *J. Orthop. Res.*, vol. 28, no. 12, pp. 1548–1553, 2010.
[37] I. Kutzner et al., "Loading of the knee joint during activities of daily living measured in vivo in five subjects," *J. Biomech.*, vol. 43, no. 11, pp. 2164–2173, 2010.
[38] I. Kutzner et al., "The effect of valgus braces on medial compartment load of the knee joint - in

vivo load measurements in three subjects," *J. Biomech*., vol. 44, no. 7, pp. 1354–1360, 2011.
[39] R. D. Komistek, J. B. Stiehl, D. A. Dennis, R. D. Paxson, and R. W. Soutas-Little, "Mathematical model of the lower extremity joint reaction forces using Kane's method of dynamics," *J. Biomech*., vol. 31, no. 2, pp. 185–189, 1997.
[40] M. O. Heller, W. R. Taylor, C. Perka, and G. N. Duda, "The influence of alignment on the musculo-skeletal loading conditions at the knee," *Langenbeck's Arch. Surg*., vol. 388, no. 5, pp. 291–297, 2003.
[41] W. R. Taylor, M. O. Heller, G. Bergmann, and G. N. Duda, "Tibio-femoral loading during human gait and stair-climbing," *J. Orthop. Res*., vol. 22, no. 3, pp. 625–632, 2004.
[42] A. Thambyah, J. C. H. Goh, and S. Das De, "Contact stresses in the knee joint in deep flexion," *Med. Eng. Phys*., vol. 27, no. 4, pp. 329–335, 2005.
[43] K. B. Shelburne, M. R. Torry, and M. G. Pandy, "Muscle, ligament, and joint-contact forces at the knee during walking," *Med. Sci. Sports Exerc*., vol. 37, no. 11, pp. 1948–1956, 2005.
[44] M. P. Shelburne, K.B., Torry M.R., Pandy, "Contributions of Muscles, Ligaments, and the Ground-Reaction Force to Tibiofemoral Joint Loading During Normal Gait," *J. Orthop. Res*., vol. 24, pp. 1983–1990, 2006.
[45] H. J. Lundberg, K. C. Foucher, and M. A. Wimmer, "A parametric approach to numerical modeling of TKR contact forces," *J. Biomech*., vol. 42, no. 4, pp. 541–545, 2009.
[46] J. N. Argenson and J. J. O'Connor, "Polyethylene wear in meniscal knee replacement. A one to nine-year retrieval analysis of the Oxford knee.," *J. Bone Joint Surg. Br*., vol. 74, no. 2, pp. 228–232, 1992.
[47] P. Plante-Bordeneuve and M. a Freeman, "Tibial high-density polyethylene wear in conforming tibiofemoral prostheses.," *J. Bone Joint Surg. Br*., vol. 75, pp. 630–636, 1993.
[48] B. J. L. Kendrick et al., "Polyethylene wear of mobile-bearing unicompartmental knee replacement at 20 years," *J. Bone Joint Surg. Br*., vol. 93–B, no. 4, pp. 470–475, 2011.
[49] A. M. Kop and E. Swarts, "Quantification of polyethylene degradation in mobile bearing knees: A retrieval analysis of the Anterior-Posterior-Glide (APG) and Rotating Platform (RP) Low Contact Stress (LCS) knee," *Acta Orthop*., vol. 78, no. 3, pp. 364–370, 2007.
[50] M. K. Harman, J. Desjardins, L. Benson, S. A. Banks, M. Laberge, and W. A. Hodge, "Comparison of polyethylene tibial insert damage from in vivo Function and in vitro wear simulation," *J. Orthop. Res*., vol. 27, no. 4, pp. 540–548, 2009.
[51] A. Srivastava, G. Y. Lee, N. Steklov, C. W. Colwell, K. A. Ezzet, and D. D. D'Lima, "Effect of tibial component varus on wear in total knee arthroplasty.," *Knee*, vol. 19, no. 5, pp. 560–3, Oct. 2012.
[52] V. Psychoyios, R. W. Crawford, and J. J. O'connor, "Wear of congruent meniscal bearings in unicompartmental knee arthroplasty," *J. Bone Joint Surg. Br*., vol. 80, pp. 876–82, 1998.
[53] J. Benjamin, J. Szivek, G. Dersam, S. Persselin, and R. Johnson, "Linear and volumetric wear of tibial inserts in posterior cruciate-retaining knee arthroplasties," *Clin. Orthop. Relat. Res*., no. 392, pp. 131–138, 2001.
[54] B. J. L. Kendrick et al., "Polyethylene wear in Oxford unicompartmental knee replacement," *J. Bone Joint Surg. Br*., vol. 92–B, no. 3, pp. 367–373, 2010.
[55] C. J. Lavernia, R. J. Sierra, D. S. Hungerford, and K. Krackow, "Activity level and wear in total knee arthroplasty: A study of autopsy retrieved specimens," *J. Arthroplasty*, vol. 16, no. 4, pp. 446–453, 2001.
[56] A. Hoshino, Y. Fukuoka, and A. Ishida, "Accurate in vivo measurement of polyethylene wear in total knee arthroplasty," *J. Arthroplasty*, vol. 17, no. 4, pp. 490–496, 2002.
[57] C. F. Kellett, A. Short, A. Price, H. S. Gill, and D. W. Murray, "In vivo measurement of total knee replacement wear C.F.," *Knee*, vol. 10, no. 11, pp. 183–187, 2004.
[58] B. J. Fregly, W. G. Sawyer, M. K. Harman, and S. A. Banks, "Computational wear prediction of a total knee replacement from in vivo kinematics.," *J. Biomech*., vol. 38, no. 2, pp. 305–14,

Feb. 2005.
[59] A.J. Price et al., "Ten-year in vivo wear measurement of a fully congruent mobile bearing unicompartmental knee arthroplasty.," *J. Bone Joint Surg. Br.*, vol. 87, no. 11, pp. 1493–1497, 2005.
[60] D. W. Murray, O. Surgeon, J. J. O 'connor, V. Psychoyios, and R. W. Crawford, "Wear of congruent meniscal bearings in unicompartmental knee arthroplasty," *J Bone Jt. Surg [Br]*, vol. 80, pp. 876–82, 1998.
[61] D. D. R. Naudie, D. J. Ammeen, G. A. Engh, and C. H. Rorabeck, "Wear and osteolysis around total knee arthroplasty," *J. Am. Acad. Orthop. Surg.*, vol. 15, no. 1, pp. 53–64, 2007.
[62] M. K. Harman, S. A. Banks, and W. A. Hodge, "Polyethylene damage and knee kinematics after total knee arthroplasty.," *Clin. Orthop. Relat. Res.*, no. 392, pp. 383–393, 2001.
[63] A. J. Carr et al., "Knee replacement," *Lancet*, vol. 379, no. 9823, pp. 1331–1340, 2012.
[64] T. McGloughlin and A. Kavanagh, "The Influence of Slip Ratios in Contemporary TKR on the Wear of Ultra-High Molecual Weight Polyethylene (UHMWPE): An Experimental View.," *J. Biomech.*, vol. 31, p. 8, 1997.
[65] H. N. Chia and B. M. Wu, "Recent advances in 3D printing of biomaterials," *J. Biol. Eng.*, vol. 9, no. 1, pp. 1–14, 2015.
[66] A. Khalyfa et al., "Development of a new calcium phosphate powder-binder system for the 3D printing of patient specific implants," *J. Mater. Sci. Mater. Med.*, vol. 18, no. 5, pp. 909–916, 2007.
[67] C. Fabry, C. Zietz, R. Dammer, and R. Bader, "12 Patterns of Wear in Total Knee Replacement," in The Unhappy Total Knee Replacement, *Cham: Springer International Publishing*, 2015, pp. 135–145.
[68] S. Affatato, L. Grillini, S. Battaglia, P. Taddei, E. Modena, and A. Sudanese, "Does knee implant size affect wear variability?," *Tribol. Int.*, vol. 66, pp. 174–181, Oct. 2013.
[69] D. Crescini, E. Sardini, and M. Serpelloni, "Design and test of an autonomous sensor for force measurements in human knee implants," *Sensors Actuators, A Phys.*, vol. 166, no. 1, pp. 1–8, 2010.
[70] K. Hébert-Losier and H. C. Holmberg, "Knee angle-specific MVIC for triceps surae EMG signal normalization in weight and non weight-bearing conditions," *J. Electromyogr. Kinesiol.*, vol. 23, no. 4, pp. 916–923, 2013.
[71] A. Cappozzo, F. Catani, A. Leardini, M. G. Benedetti, and U. Della Croce, "Position and orientation in space of bones during movement: Experimental artefacts," *Clin. Biomech.*, vol. 11, no. 2, pp. 90–100, 1996.
[72] F. B. Holness and A. Price, "Additive Manufacturing Process of 3D Polyaniline Transducers via Direct Ink Writing," no. September, 2017.
[73] F. B. Holness and A. D. Price, "Direct ink writing of 3D conductive polyaniline structures and rheological modelling," *Smart Mater. Struct.*, vol. 27, no. 1, 2018.
[74] Z. Wang et al., "Three-Dimensional Printing of Polyaniline/Reduced Graphene Oxide Composite for High-Performance Planar Supercapacitor," *ACS Appl. Mater. Interfaces*, vol. 10, no. 12, pp. 10437–10444, 2018.
[75] D. D. D'Lima, N. Steklov, B. J. Fregly, S. A. Banks, and C. W. Colwell, "In vivo contact stresses during activities of daily living after knee arthroplasty," *J. Orthop. Res.*, vol. 26, no. 12, pp. 1549–1555, 2008.
[76] Ancientart, "Anatomy Movement Knee," 2017. [Online]. Available: http://ancientart.co/ad49ff/anatomy-movement-knee. [Accessed: 24-Mar-2018].
[77] OrthoInfo, "Knee Replacement Implants." [Online]. Available: https://orthoinfo.aaos.org/en/treatment/knee-replacement-implants/. [Accessed: 04-Apr-2018].
[78] U.S. Department of Justice, "Analytical Balance Mettler," 2002. .
[79] Inspecs, "Coordinate Measuring Machine," 2016. .
[80] Florida Hospital, "Micro CT knee insert," 2016. .
[81] Verdonk, "Osteotomie." [Online]. Available: http://www.verdonk.be/osteotomie.html. [Accessed: 24-Mar-2018].

APPENDIX

Appendix A - Technical drawing connection part

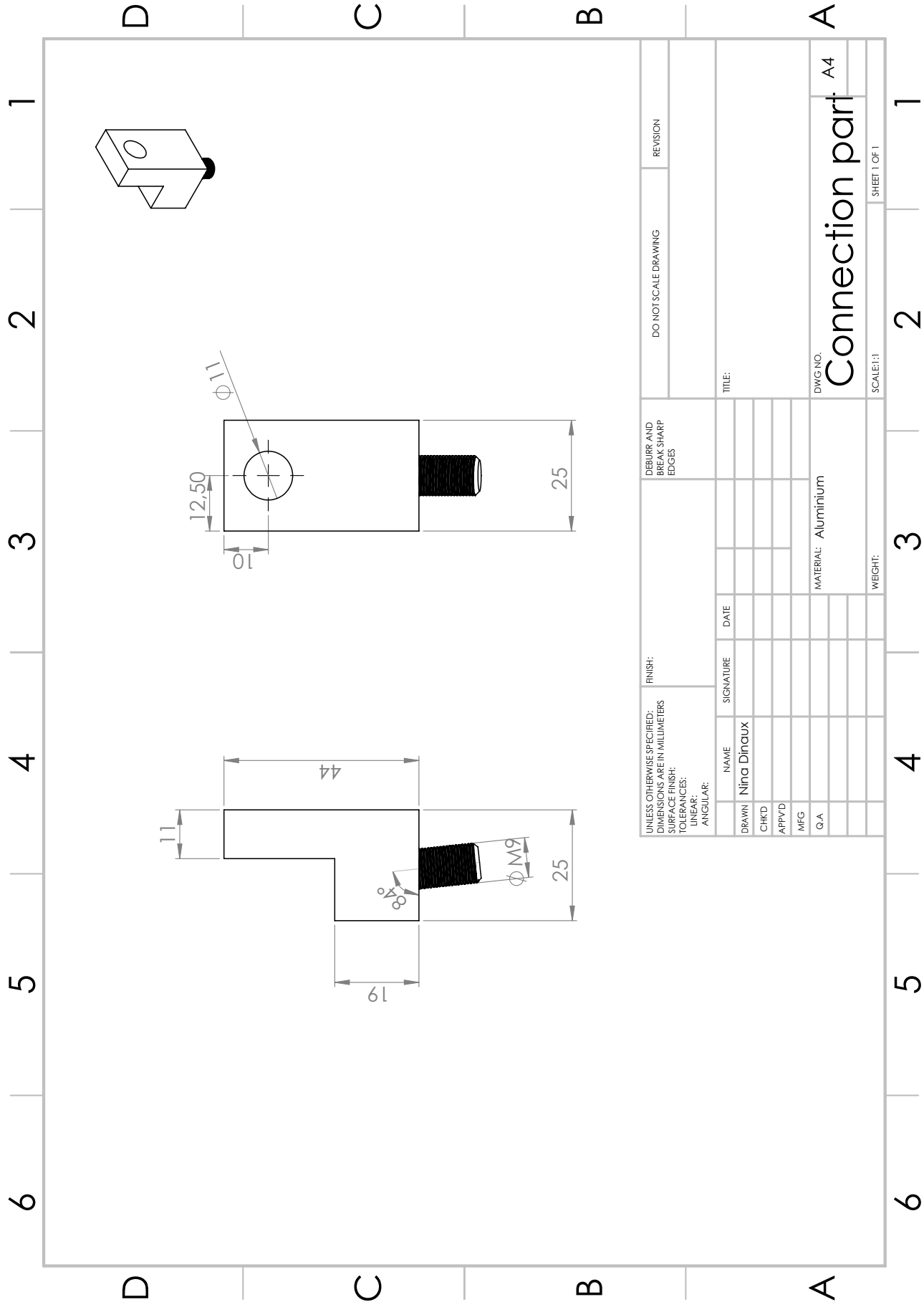

Appendix B - Technical drawing tibial component

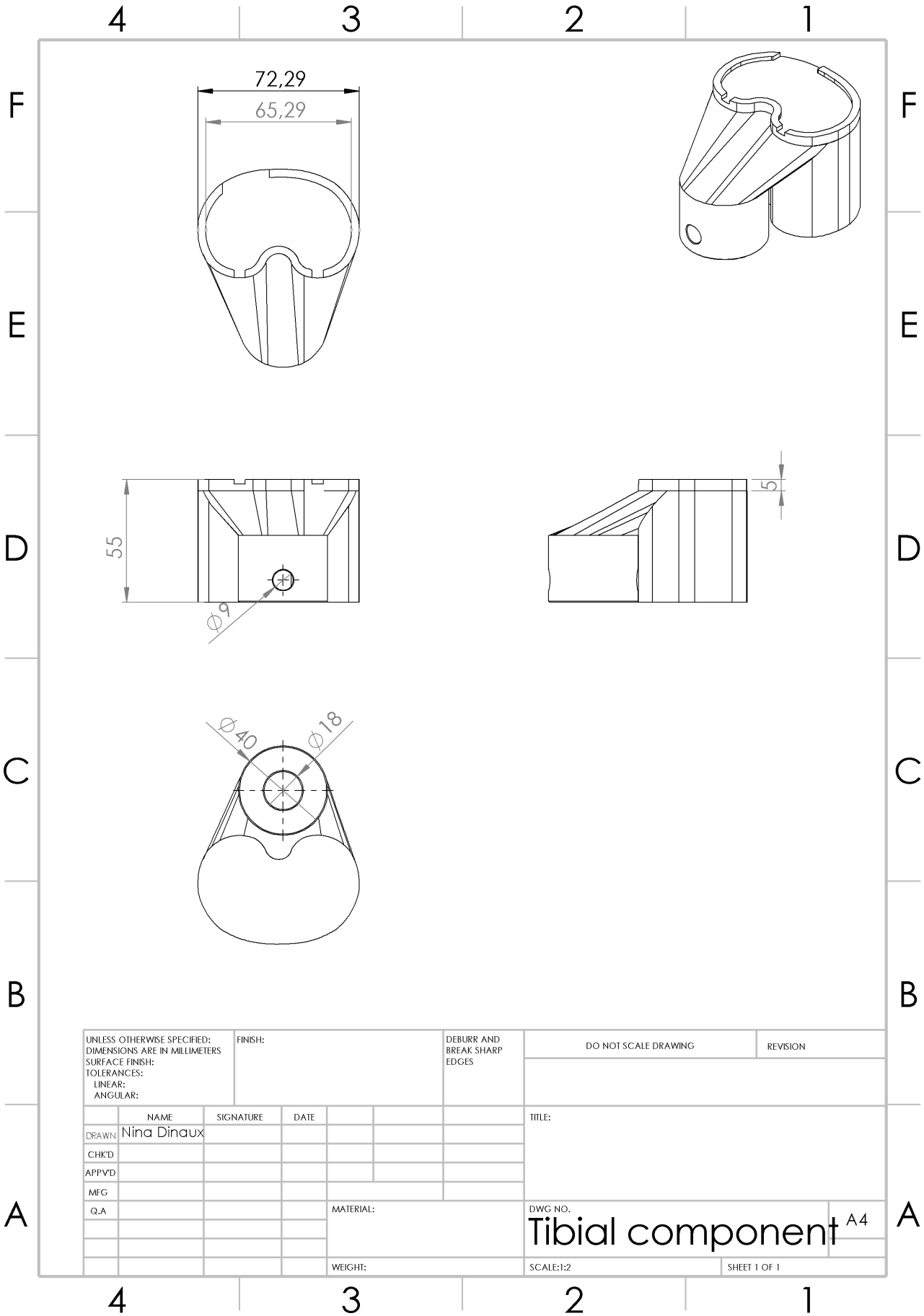

Appendix C - Technical drawings slices wear measuring insert

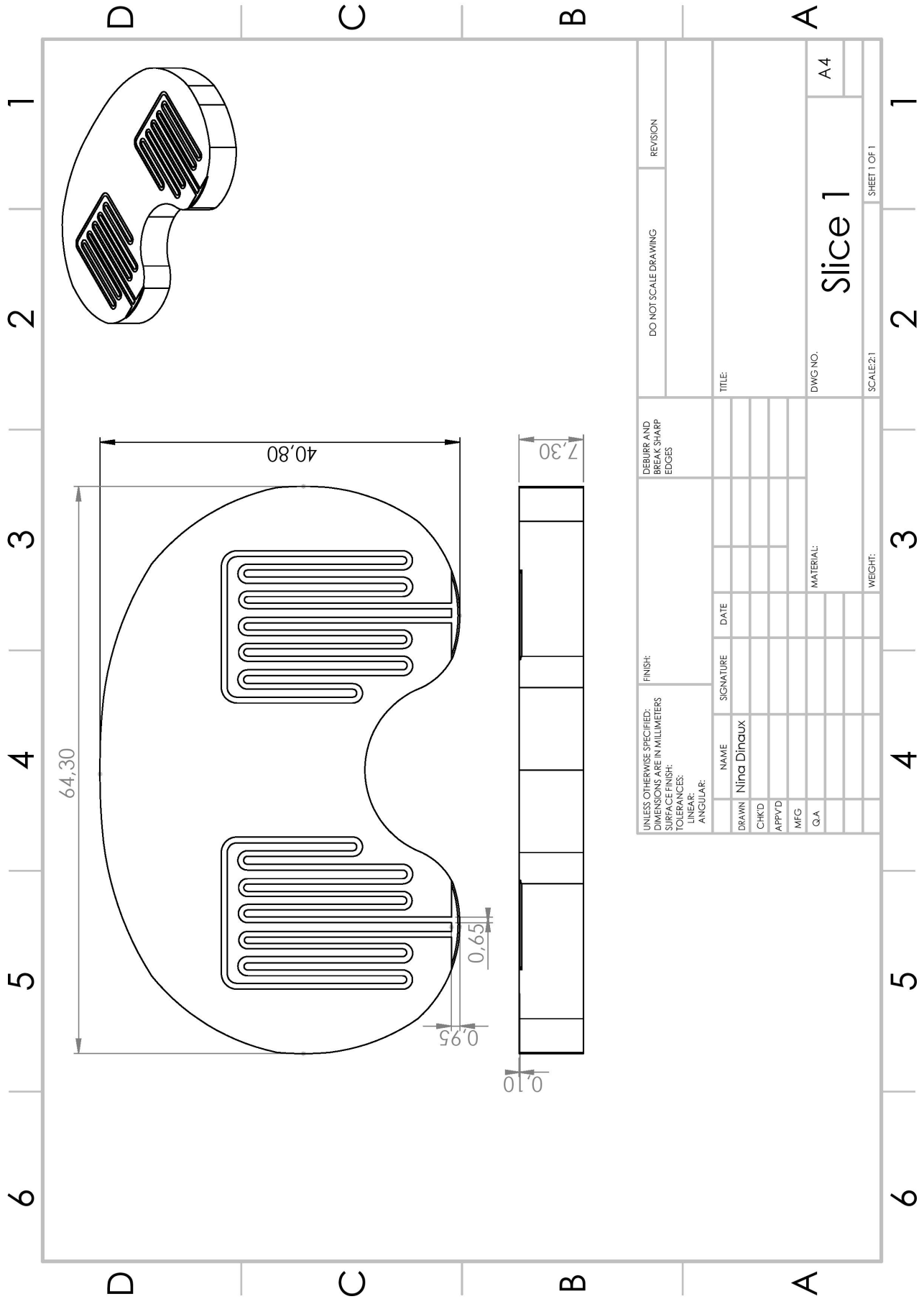

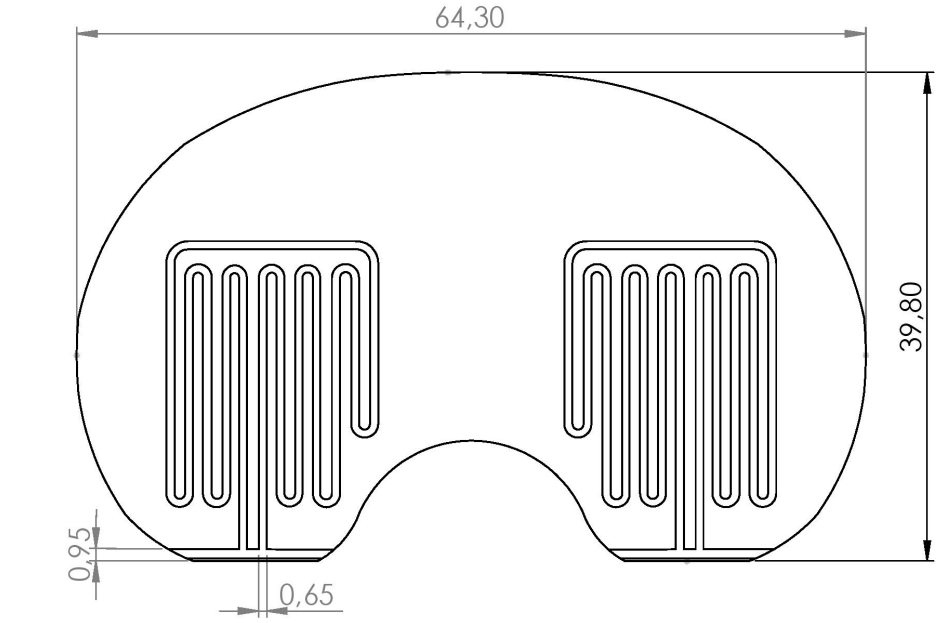

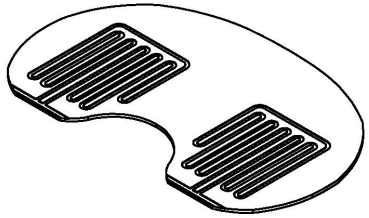

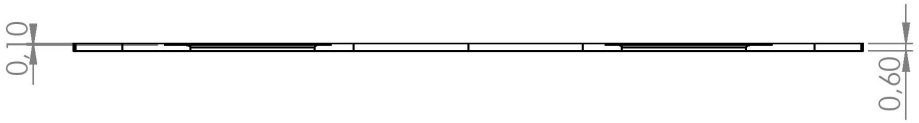

UNLESS OTHERWISE SPECIFIED: DIMENSIONS ARE IN MILLIMETERS SURFACE FINISH: TOLERANCES: LINEAR: ANGULAR:		FINISH:		DEBURR AND BREAK SHARP EDGES		DO NOT SCALE DRAWING	REVISION
	NAME	SIGNATURE	DATE				
DRAWN	Nina Dinaux					TITLE:	
CHK'D							
APPV'D							
MFG							
Q.A				MATERIAL:		DWG NO. Slice 2	A4
				WEIGHT:		SCALE:2:1	SHEET 1 OF 1

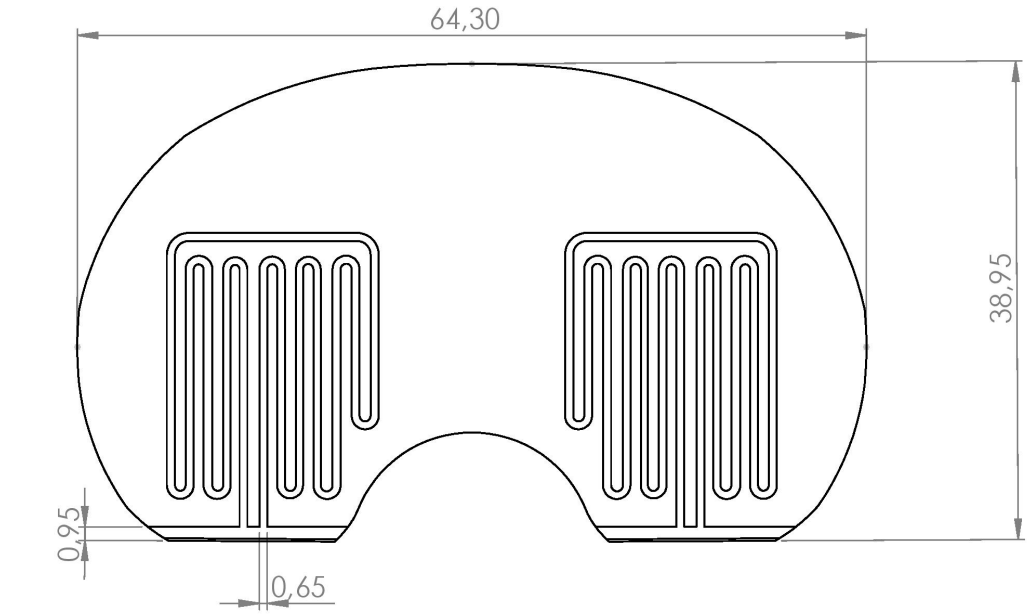

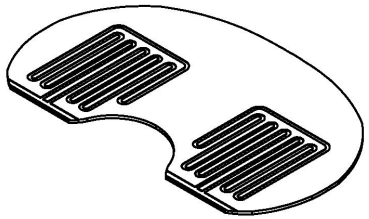

UNLESS OTHERWISE SPECIFIED: DIMENSIONS ARE IN MILLIMETERS SURFACE FINISH: TOLERANCES: LINEAR: ANGULAR:		FINISH:		DEBURR AND BREAK SHARP EDGES		DO NOT SCALE DRAWING	REVISION
	NAME	SIGNATURE	DATE			TITLE:	
DRAWN	Nina Dinaux						
CHK'D							
APPV'D							
MFG							
Q.A				MATERIAL:		DWG NO. Slice 3	A4
				WEIGHT:		SCALE:2:1	SHEET 1 OF 1

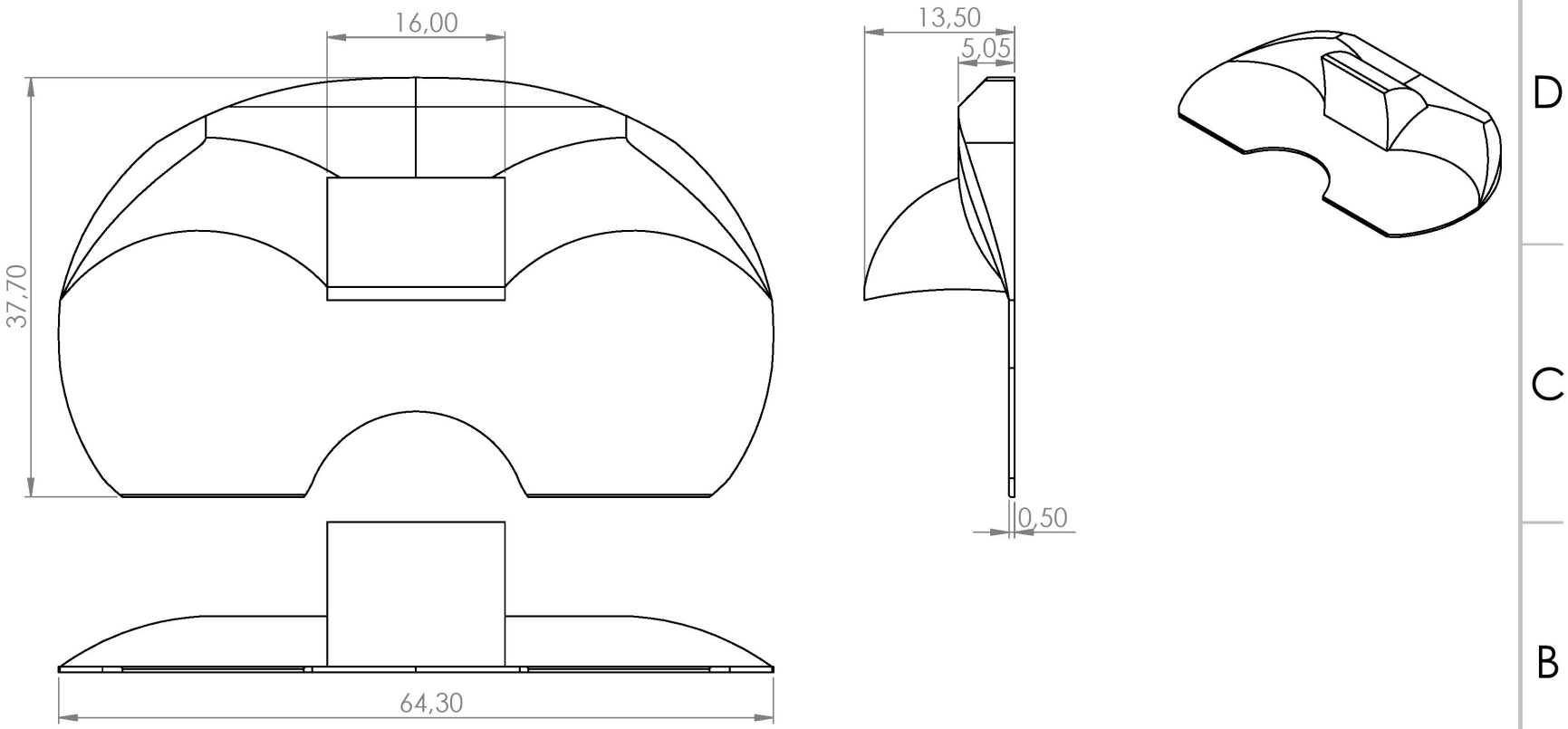

UNLESS OTHERWISE SPECIFIED: DIMENSIONS ARE IN MILLIMETERS SURFACE FINISH: TOLERANCES: LINEAR: ANGULAR:	FINISH:		DEBURR AND BREAK SHARP EDGES	DO NOT SCALE DRAWING	REVISION		
	NAME	SIGNATURE	DATE				TITLE:
DRAWN	Nina Dinaux						
CHK'D							
APPV'D							
MFG							
Q.A				MATERIAL:			DWG NO. Slice 4
							A4
				WEIGHT:		SCALE:2:1	SHEET 1 OF 1

Appendix D - Graphs resistance sensors

To improve the readability of the graphs, next to each graph a visualization of the sensor the graph is concerning to is shown.

Test 1
The outputs of sensor 2-2, 2-6, 3-2 and 3-6 can be found in Figure D-1 to D-4 respectively. All other sensors gave an output of infinite.

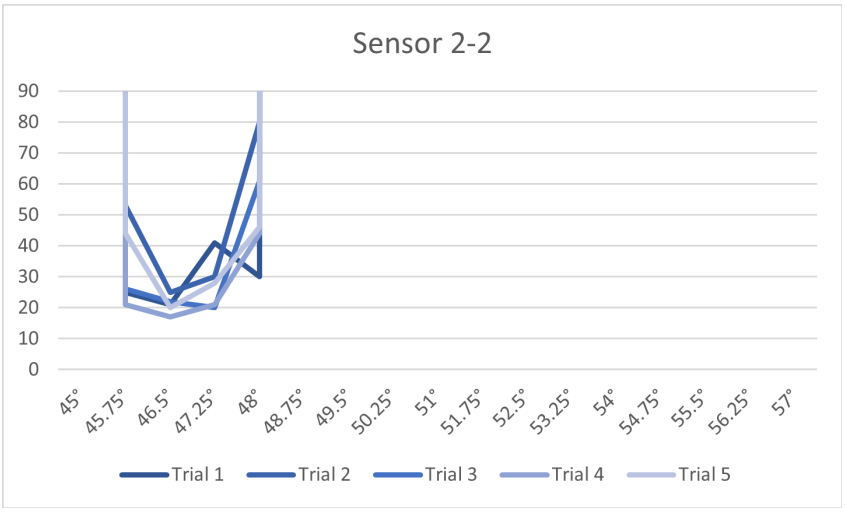

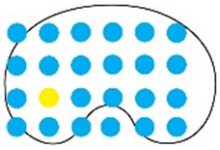

Figure D - 1 – Output of sensor 2-2 in test 1

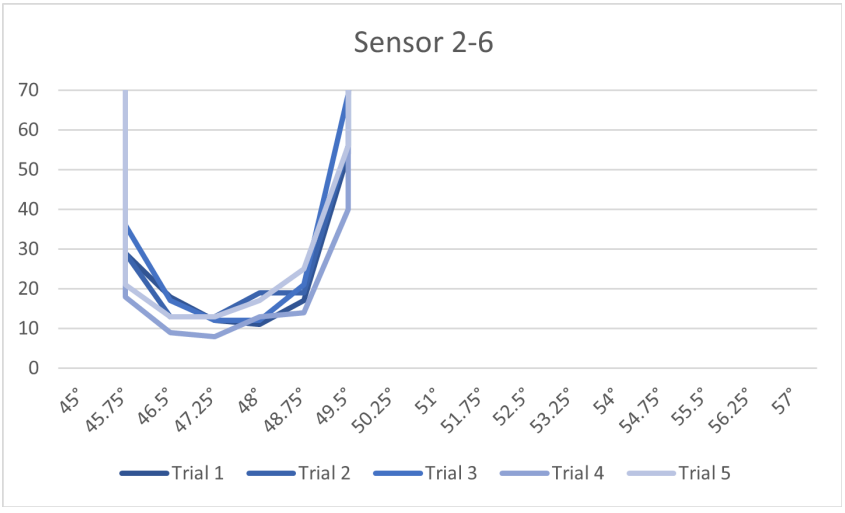

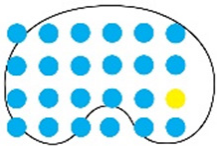

Figure D - 2 - Output of sensor 2-6 in test 1

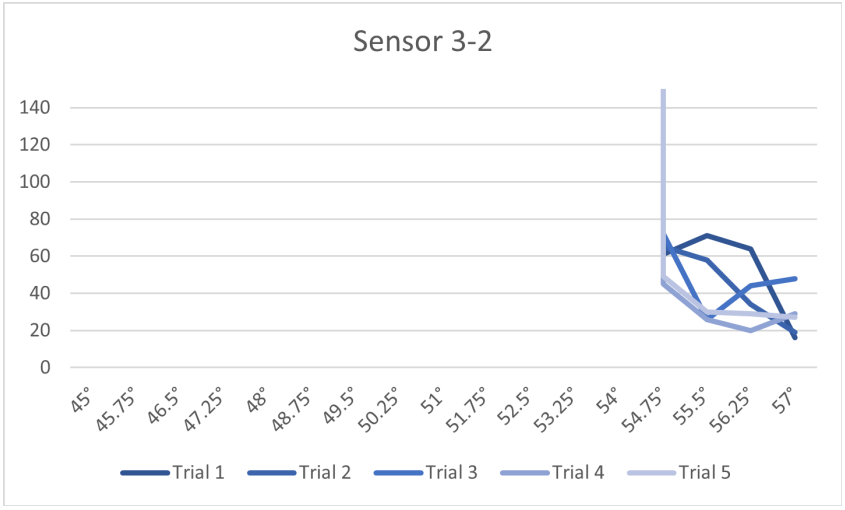

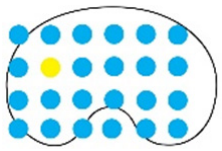

Figure D - 3 - Output of sensor 3-2 in test 1

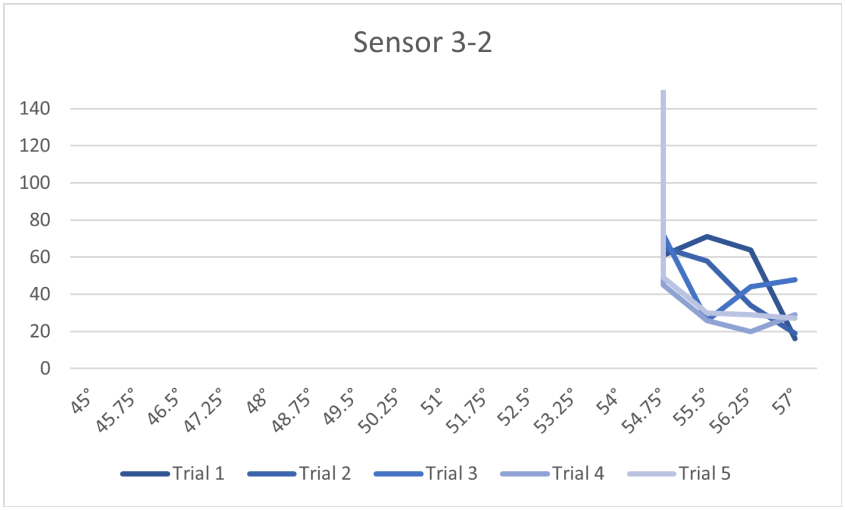

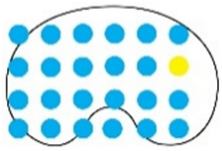

Figure D - 4 – Output of sensor 3-6 in test 1.

Test 2

The outputs of sensor 2-2 and 2-6 can be found in Figure D-5 to D-6 respectively. All other sensors gave an output of infinite.

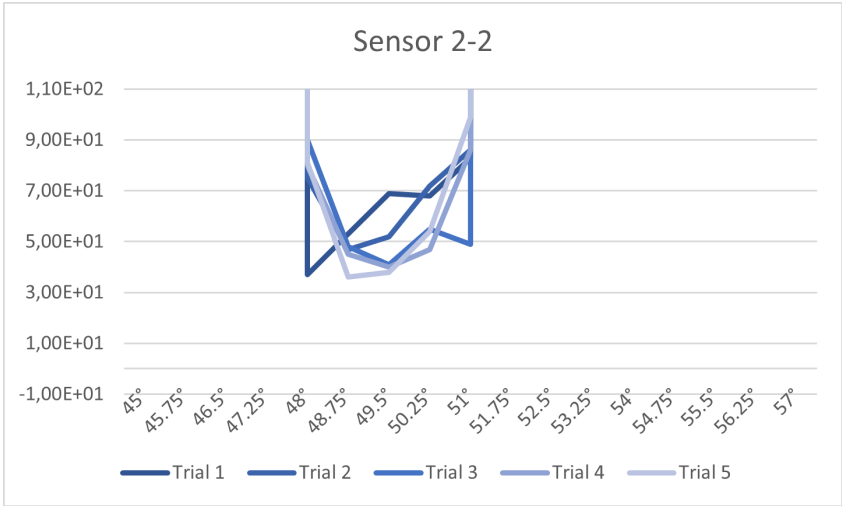

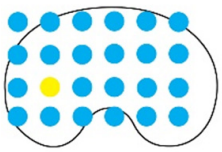

Figure D - 5 – Output of sensor 2-2 in test 2

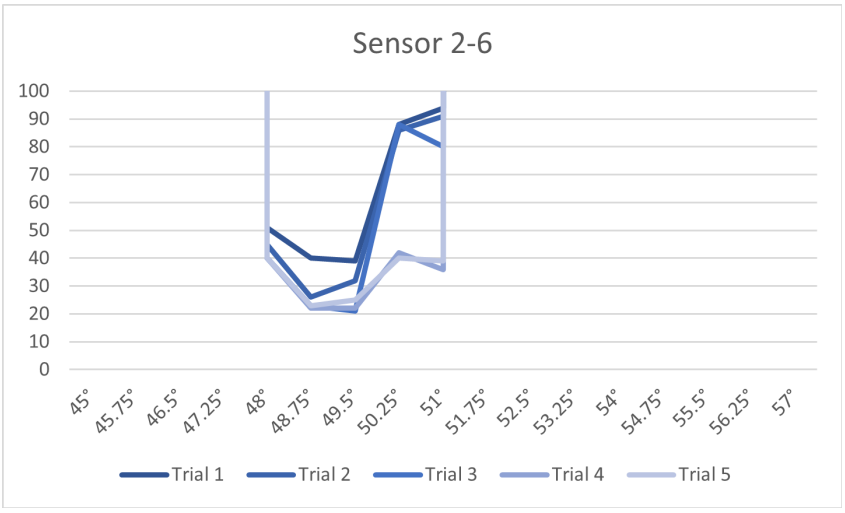

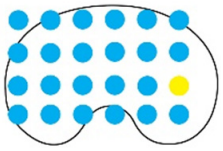

Figure D - 6 – Output of sensor 2-6 in test 2

Test 3

The outputs of sensor 2-1 and 2-5 can be found in Figures D-7 to D-8 respectively. All other sensors gave an output of infinite.

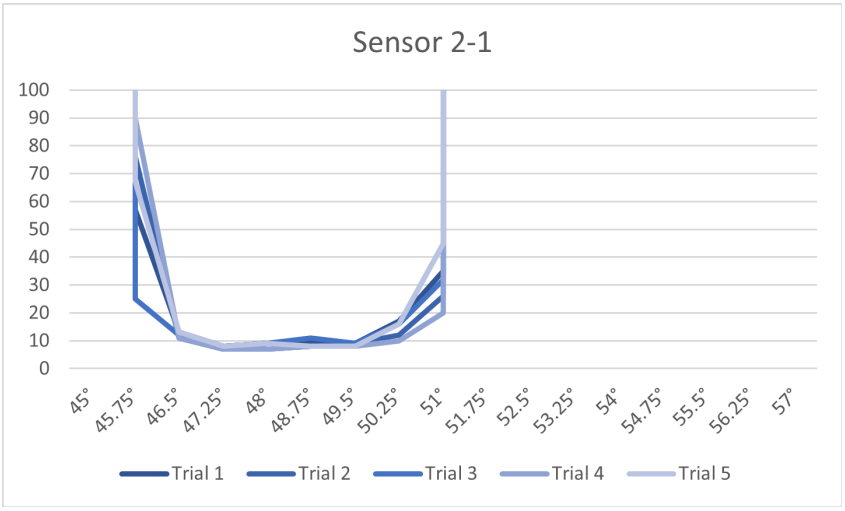

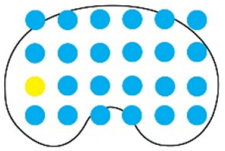

Figure D - 7 – Output of sensor 2-1 in test 3

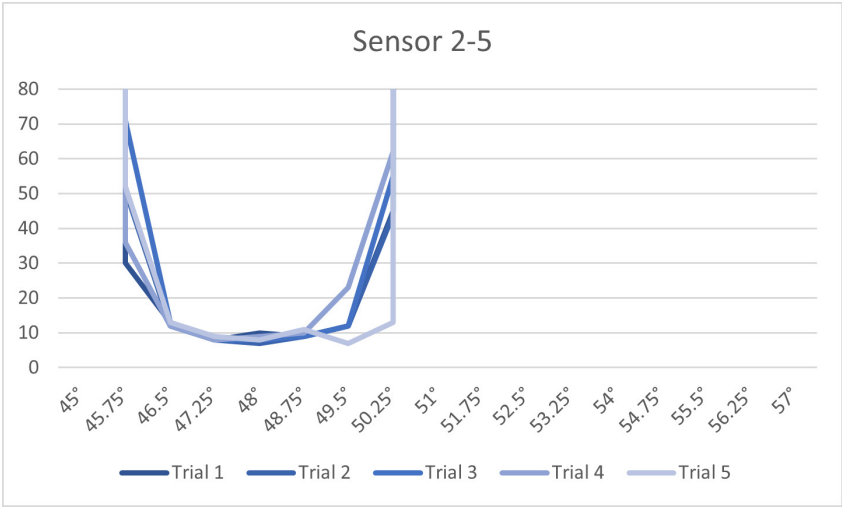

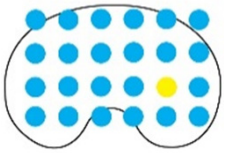

Figure D - 8 – Output of sensor 2-5 in test 3

Test 4

The outputs of sensor 2-1, 2-5, 3-1 and 3-5 can be found in Figure D-9 to D-12 respectively. All other sensors gave an output of infinite.

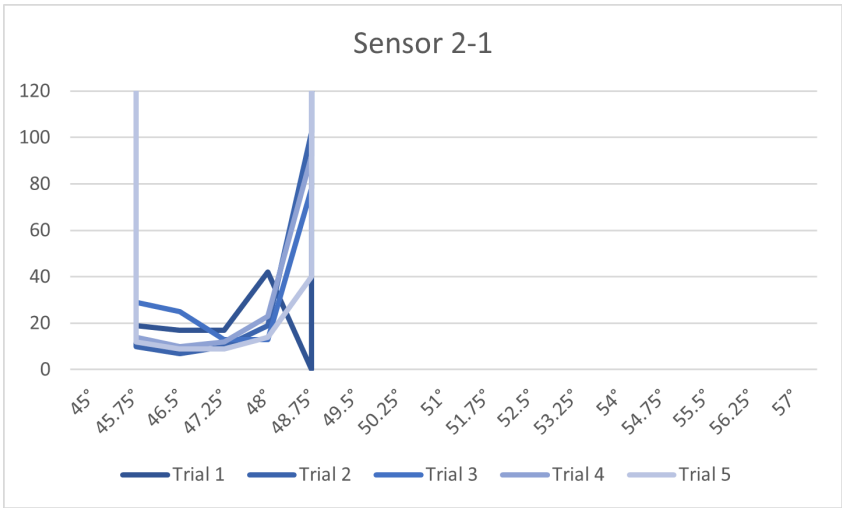

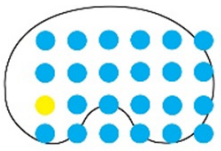

Figure D - 9 – Output of sensor 2-1 in test 4

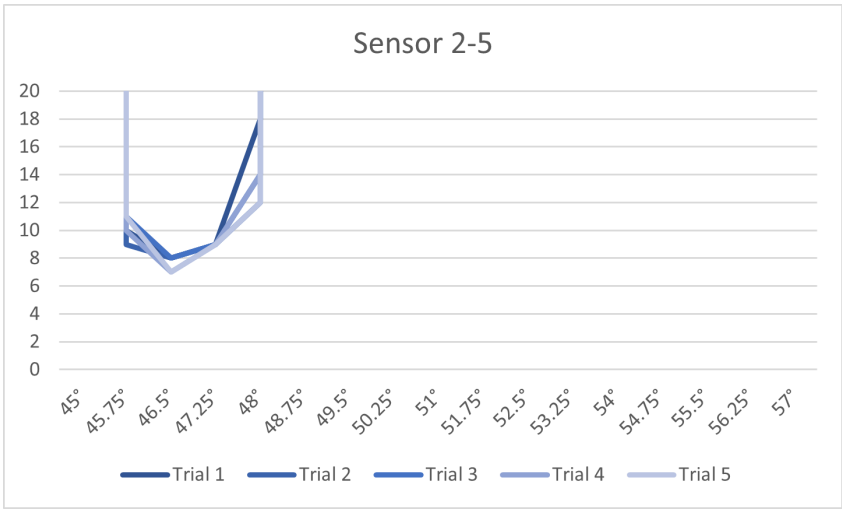

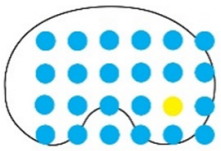

Figure D - 10 – Output of sensor 2-5 in test 4

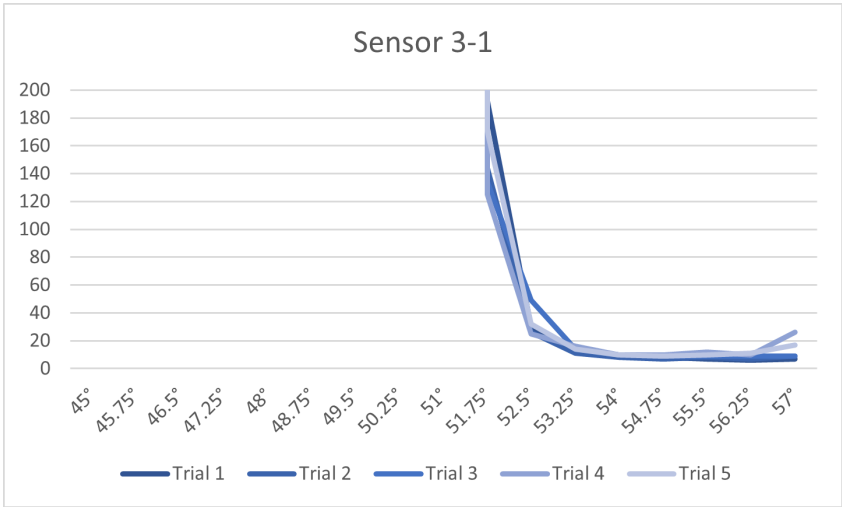

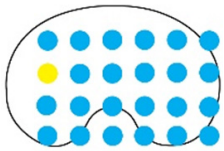

Figure D - 11 – Output of sensor 3-1 in test 4

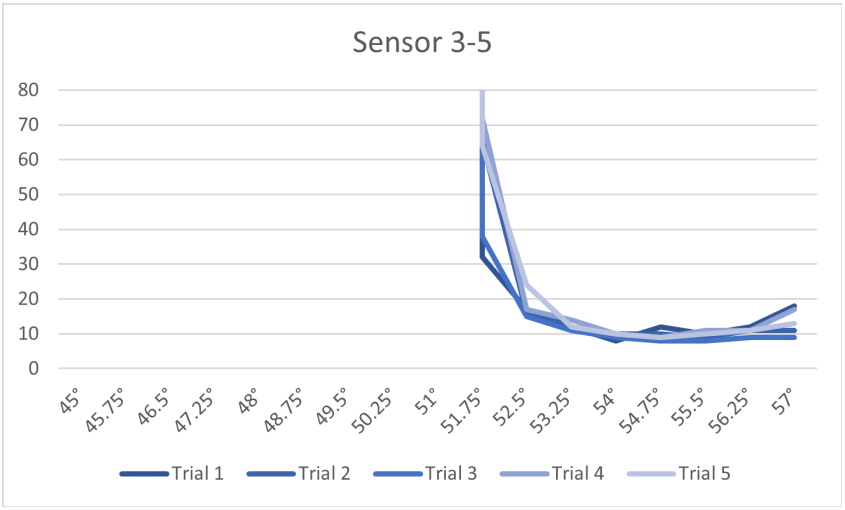

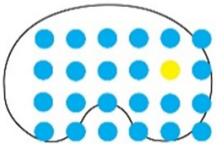

Figure D - 12 – Output of sensor 3-5 in test 4

Appendix E - Technical drawing of assembly wear measuring insert

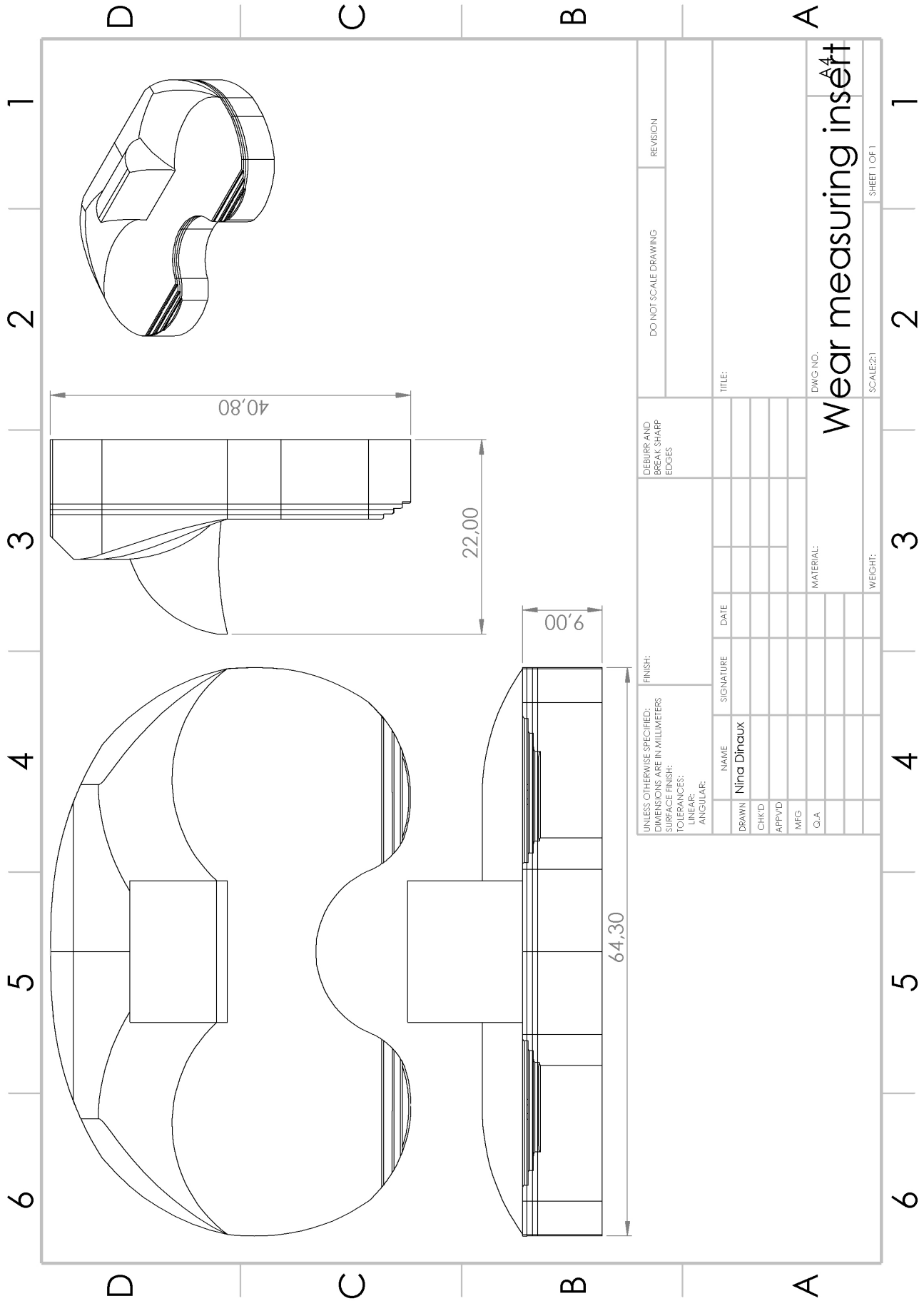

Master Thesis
N.M. Dinaux
Biomedical Engineering
Technical University of Delft
2018